Supporting Information

For

Nitric oxide reactivity of copper(II) complexes of bidentate amine ligands: Effect of chelate ring size on the stability of [Cu^{II}-NO] intermediate

Moushumi Sarma[a], Vikash Kumar[a], Aswini Kalita[a], Ramesh C. Deka[b], Biplab Mondal[a*]

[a]*Department of Chemistry, Indian Institute of Technology Guwahati, Assam 781039, India*

[b]*Department of Chemical Sciences, Tezpur University, Napaam, Tezpur – 784 028, Assam, India*

E-mail: biplab@iitg.ernet.in

Table of Contents	**Page**

Synthesis of ligands L_2:

The ligand $\mathbf{L_2}$ was synthesized using the following procedure.

Ligand $\mathbf{L_2}$ was synthesized in three steps (scheme S1):

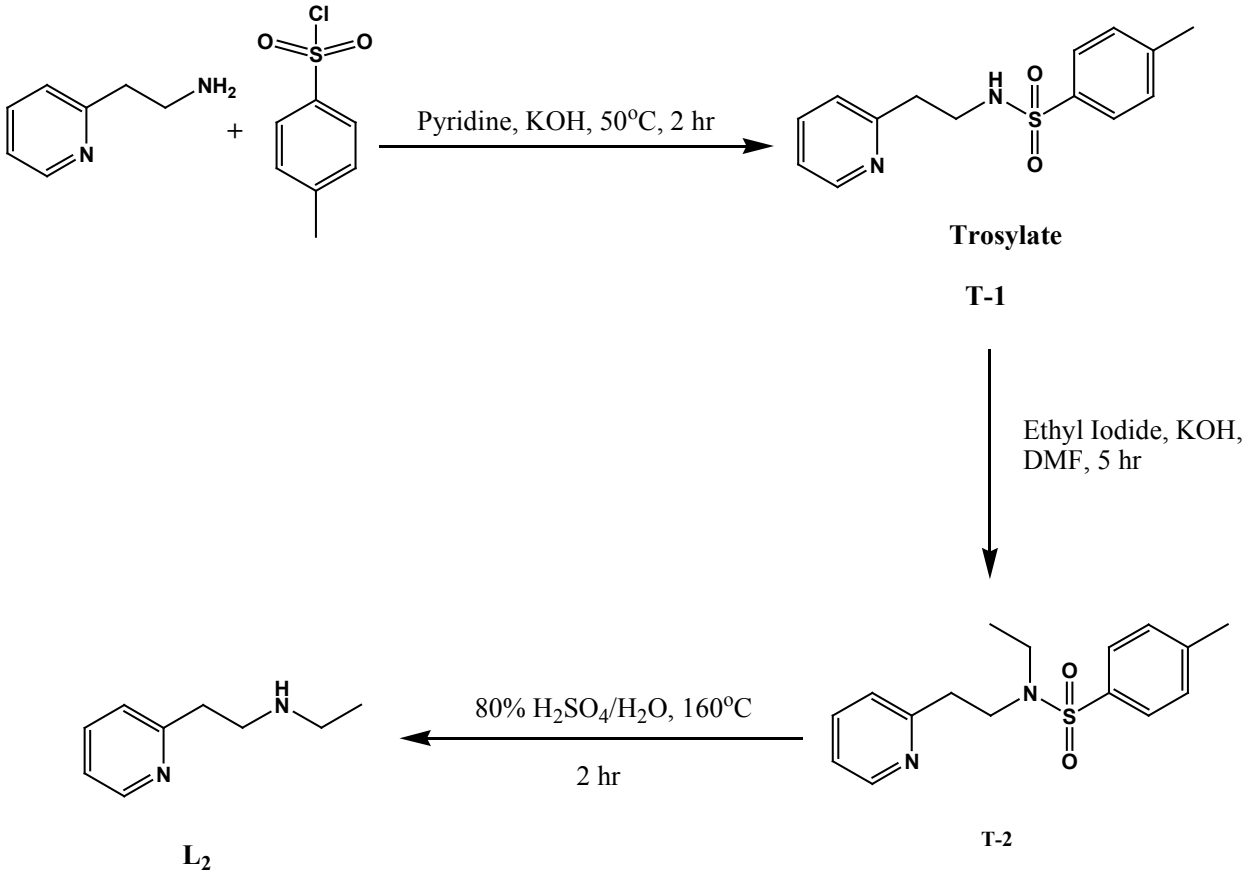

Scheme S1

Step I. Tosylation of 2-(2-aminoethyl)-pyridine:

A 250-ml two-necked round-bottomed flask equipped with a magnetic stirring bar, reflux condenser and a rubber septum was charged with 2-(2-aminoethyl)-pyridine (0.736 g; 6 mmol), pyridine (20 ml) and potassium hydroxide (1.01 g; 18 mmol). The mixture was stirred and cooled in an ice bath while 3.43 g (18 mmol) of tosyl chloride was added over a period of 5 min. After 5 min, the ice bath was removed and the reaction mixture was heated to 50 °C in an oil

bath for 2 h with constant stirring. The reaction mixture was allowed to cool to room temperature was then poured into 20 ml ice-cold water. The crude tosylated product was obtained as whitish precipitate. The precipitate was purified by column chromatography using hexane to give 1.45 g (~ 87%) of 2-(N-*p*-methylbenzenesulfonamide-2-aminoethyl)-pyridine (**T-1**). FT-IR: 3064(m), 1597(m), 1325(s), 1156(m), 1082(s), 550(s) cm^{-1}. ^{1}H-NMR (400 MHz, $CDCl_3$): δ_{ppm} 8.43(d, 1H), 7.70(d, 2H), 7.55(t, 1H), 7.24(d, 2H), 7.11(t, 1H), 7.05(d,1H), 3.32(q, 2H), 2.90(t, 2H), 2.37(s, 3H) . ^{13}C-NMR (100 MHz, $CDCl_3$): δ_{ppm}, 159.04, 149.19, 143.30, 137.32, 136.93, 129.79, 127.22, 123,72, 121.92, 42.43, 36.42, 21.65. (m+23)/z: calculated 299.07 found 299.14.

Step II: Ethylation of T-1:

A 250-ml two-necked round-bottomed flask equipped with a magnetic stirring bar, reflux condenser and a rubber septum was charged with 0.829 g (3 mmol) of **T-1,** 1.1 g (21 mmol) of potassium hydroxide, and 20 ml of anhydrous dimethylformamide (DMF). To this 2 g (12 mmol) ethyl iodide was added over a period of 5 min and the resulting mixture was heated at 60 °C in an oil bath for 4h. The reaction mixture was then allowed to cool to room temperature, diluted with 250 ml of water, and extracted with $CHCl_3$ (100 ml x 3 portions). The combined organic extracts were washed with brine (100 ml), dried over anhydrous sodium sulphate and concentrated under reduced pressure to give pale yellow oil. The oil was purified by column chromatography on neutral alumina to give 0.69 g (~86%) of **T-2** as a viscous pale yellow liquid. FT-IR: 2925(m), 1594(m), 1336(s), 1156(s), 550(s) cm^{-1}. ^{1}H-NMR (400 MHz, $CDCl_3$): δ_{ppm} 8.46(d, 1H), 7.65(d, 2H), 7.56(t, 1H), 7.24(d, 2H), 7.16(d, 1H), 7.08(t, 1H), 3.47(t, 2H), 3.16(q, 2H), 3.02(t, 2H), 2.12(s. 2H), 0.99(t, 3H). ^{13}C-NMR (100 MHz, $CDCl_3$): δ_{ppm}, 156.65, 149.30, 143.19, 136.98, 136.58, 129.65, 127.11, 123.76, 121.64, 47.50, 43.421, 38.07, 21.48, 13.91. (m+1)/z: calculated 305.12 Found 305.18.

Step III. Hydrolysis of T-2:

A 100-ml two-necked round-bottomed flask equipped with a magnetic stirring bar, reflux condenser, and a rubber septum was charged with 3.04g (10 mmol) of **T-2**, 17 ml of 80% H_2SO_4, and the resulting mixture was heated at 160 °C in an oil bath with constant stirring till solid goes into solution. The reaction mixture was then allowed to cool to room temperature, diluted with 30 ml of water and neutralized with 20% NaOH solution. The resulting amine was then extracted with 3 x 50 ml portions of dichloromethane. The combined organic extracts were washed with brine (100 ml), dried over anhydrous sodium sulphate and concentrated under reduced pressure. The residue was purified by column chromatography on neutral alumina to give 0.65 g (~43%) of the desired amine $\mathbf{L_2}$. FT-IR: 297(m), 1595(m), 1382(s) cm^{-1}. ^{1}H-NMR (400 MHz, $CDCl_3$): δ_{ppm}: 8.48(d,1H), 7.56(t, 1H), 7.15(d, 1H), 7.08(t, 1H), 3.02(t, 2h), 2.99(t, 2H),2.70(q,2H), 1.09(t, 2H). ^{13}C-NMR (100 MHz, CDCl3): δ_{ppm} 49159.75, 148.75, 135.81, 122.73, 120.56, 48.69, 43.42, 37.92, 14.71; (m+1)/z: calculated 151.12 found 151.11.

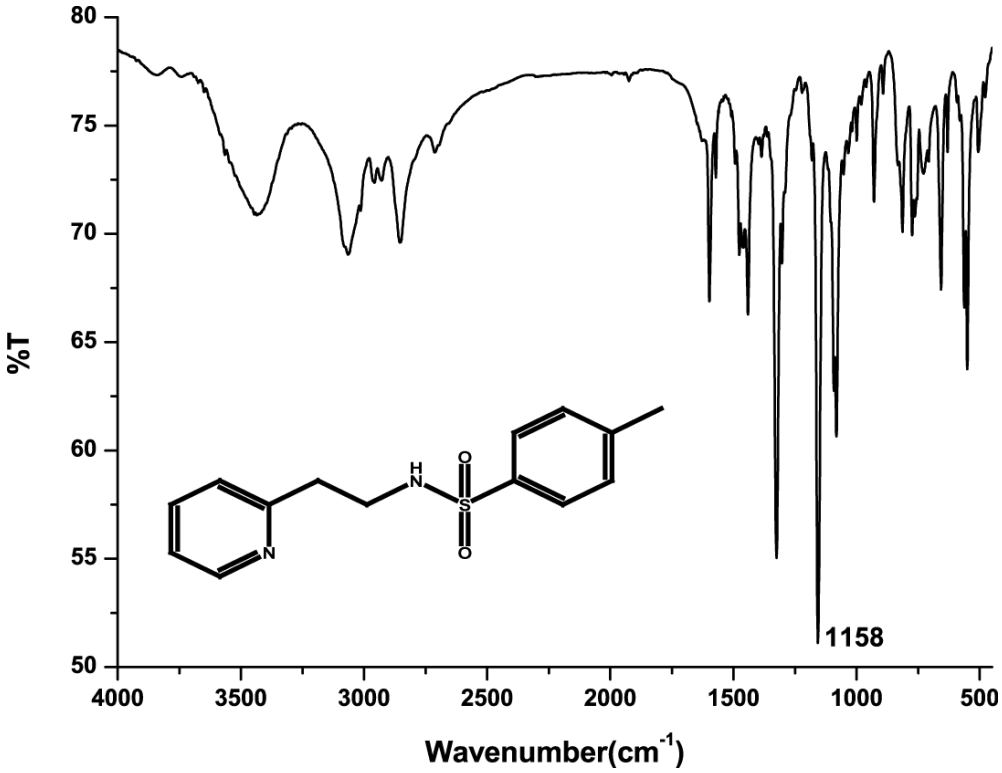

Figure S1: FT-IR spectrum of **T-1** in KBr pellet.

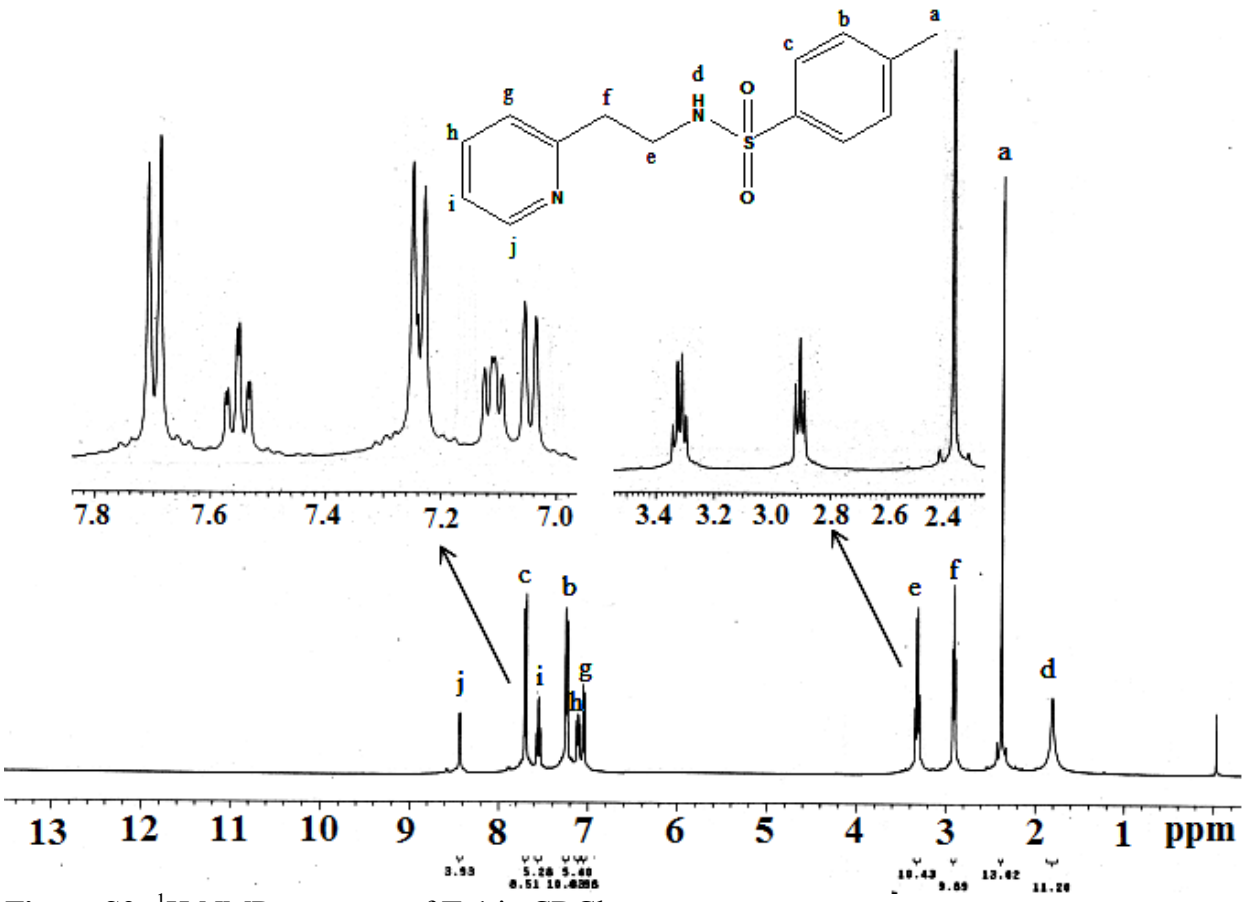

Figure S2: ^{1}H-NMR spectrum of **T-1** in $CDCl_3$.

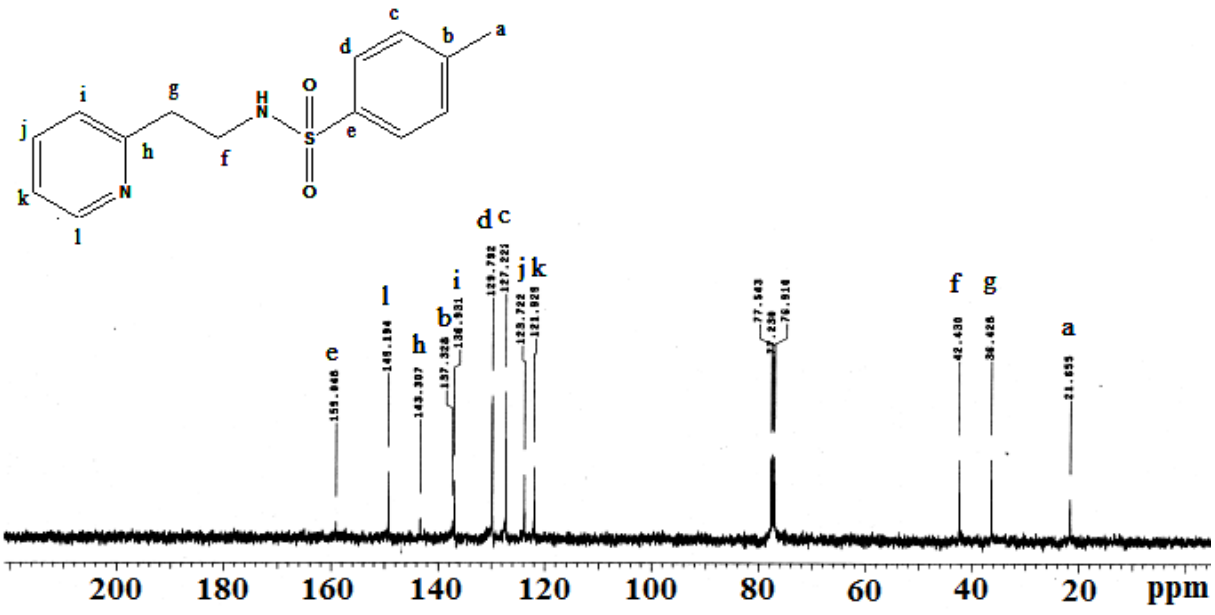

Figure S3: ^{13}C-NMR spectrum of **T-1** in $CDCl_3$.

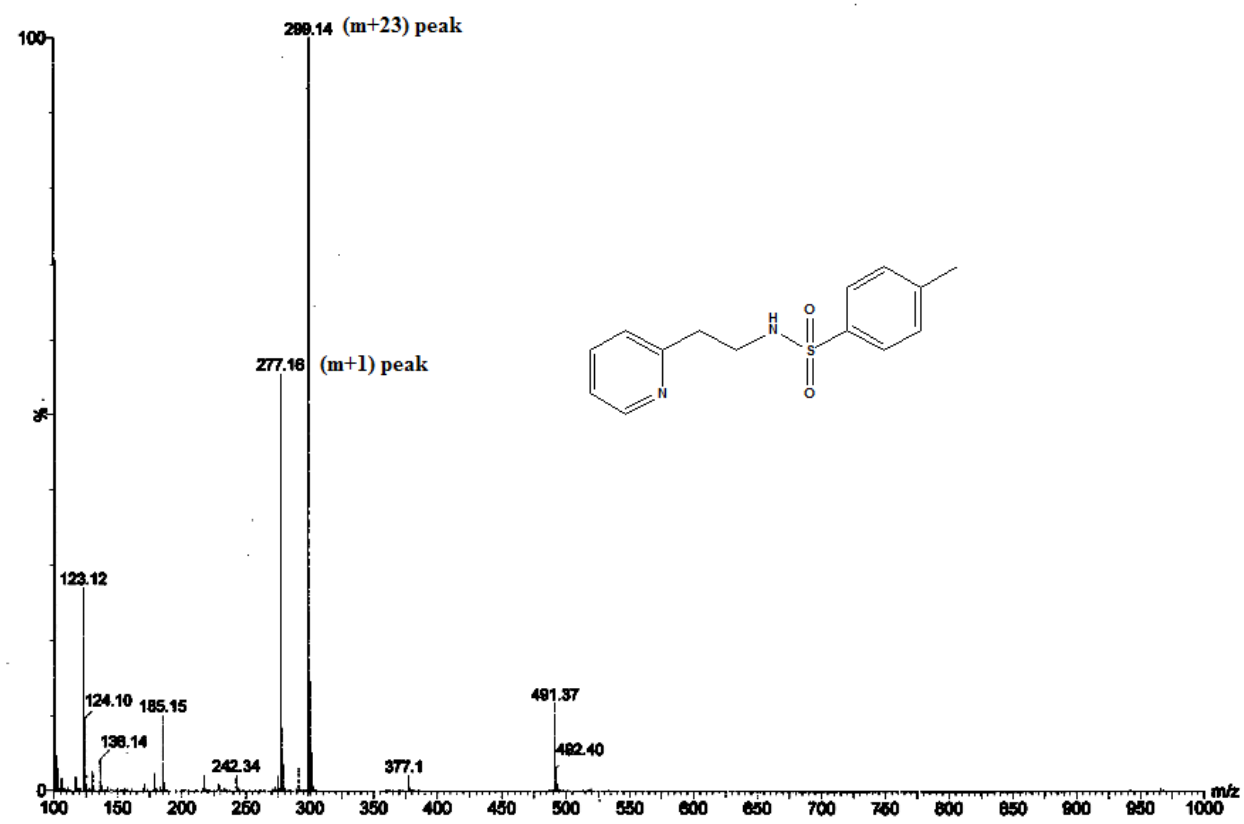

Figure S4: ESI-Mass spectrum of **T-1** in methanol.

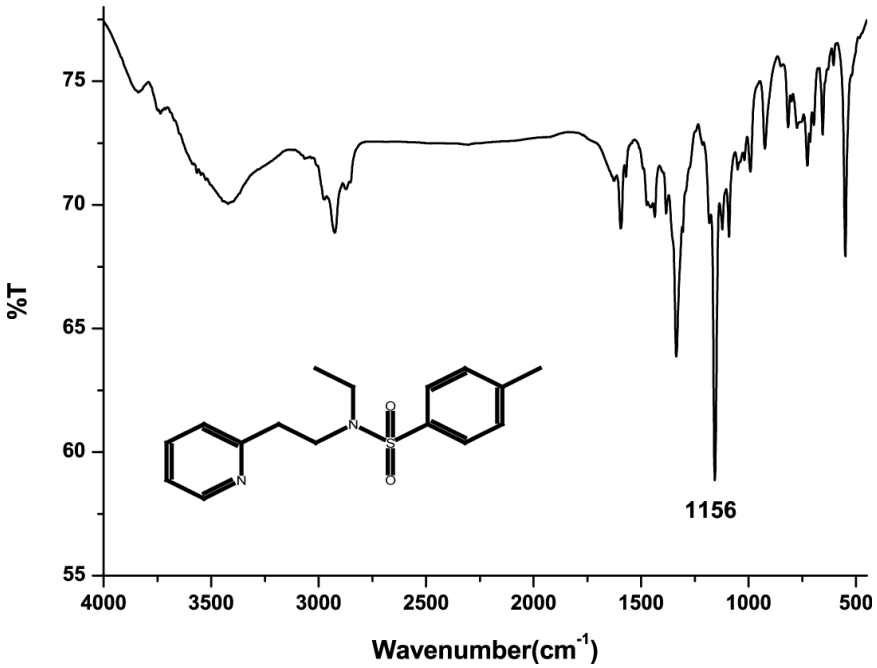

Figure S5: FT-IR spectrum of **T-2** in KBr pellet.

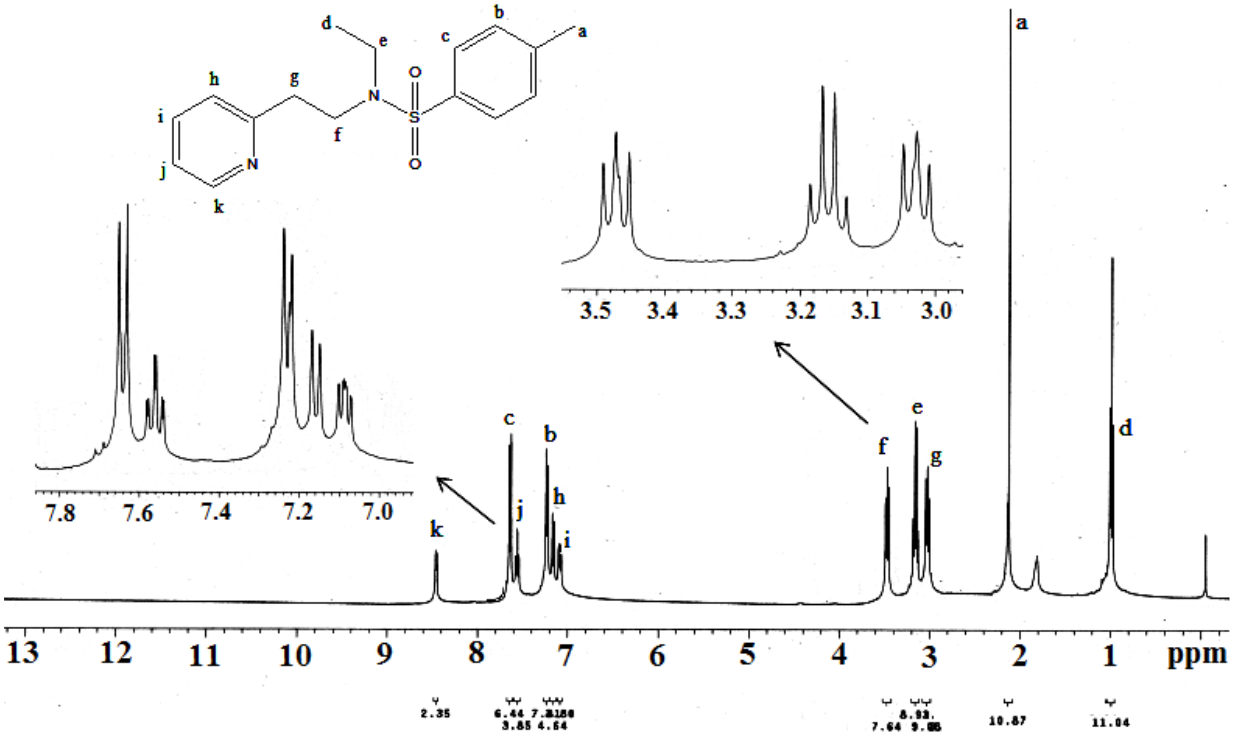

Figure S6: ^{1}H-NMR spectrum of **T-2** in $CDCl_3$.

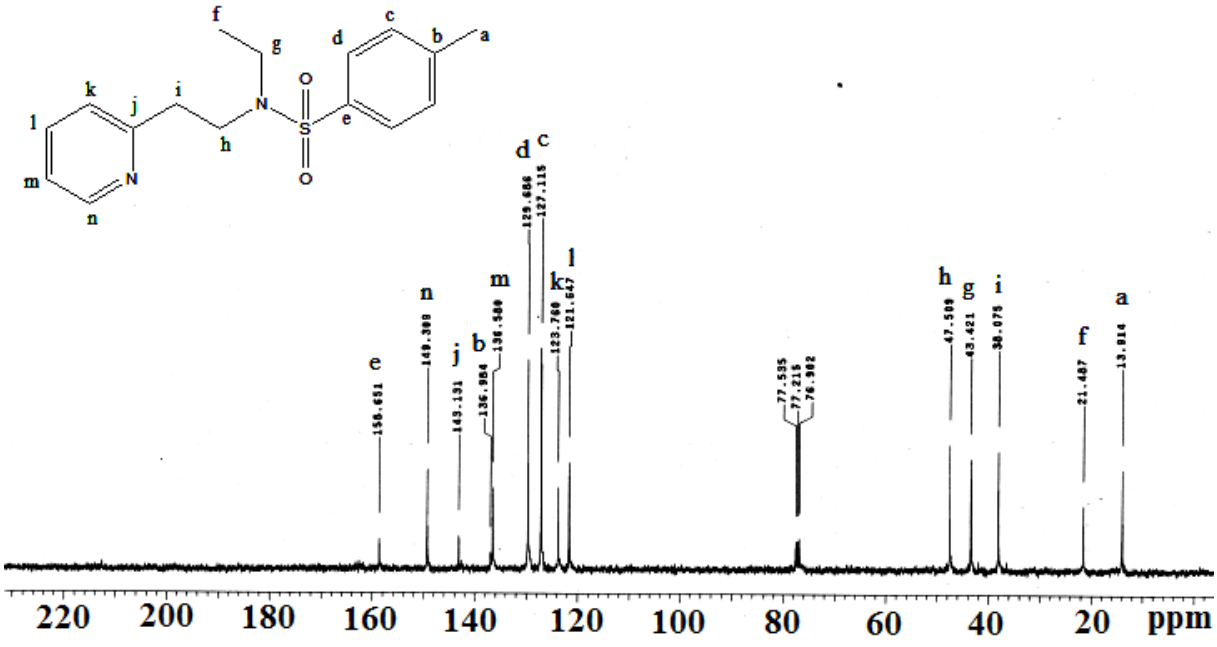

Figure S7: ^{13}C-NMR spectrum of **T-2** in $CDCl_3$.

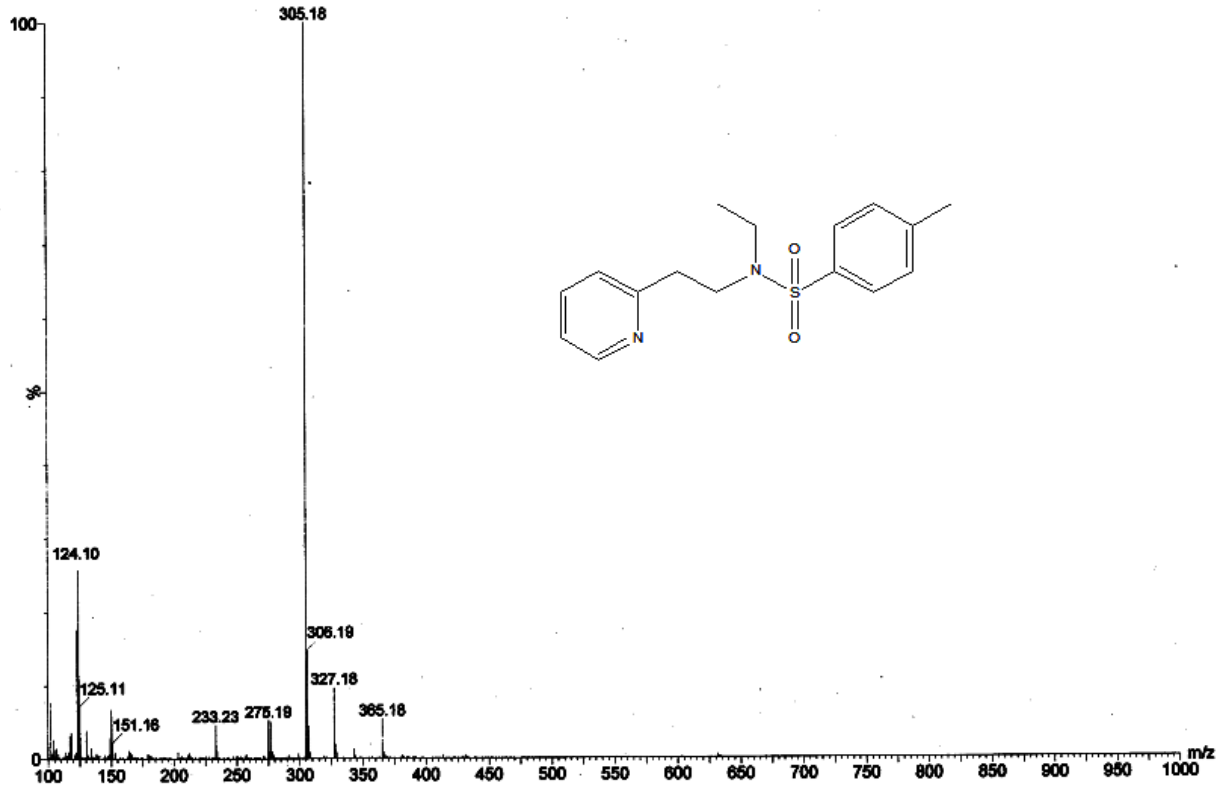

Figure S8: ESI-Mass spectrum of **T-2** in methanol.

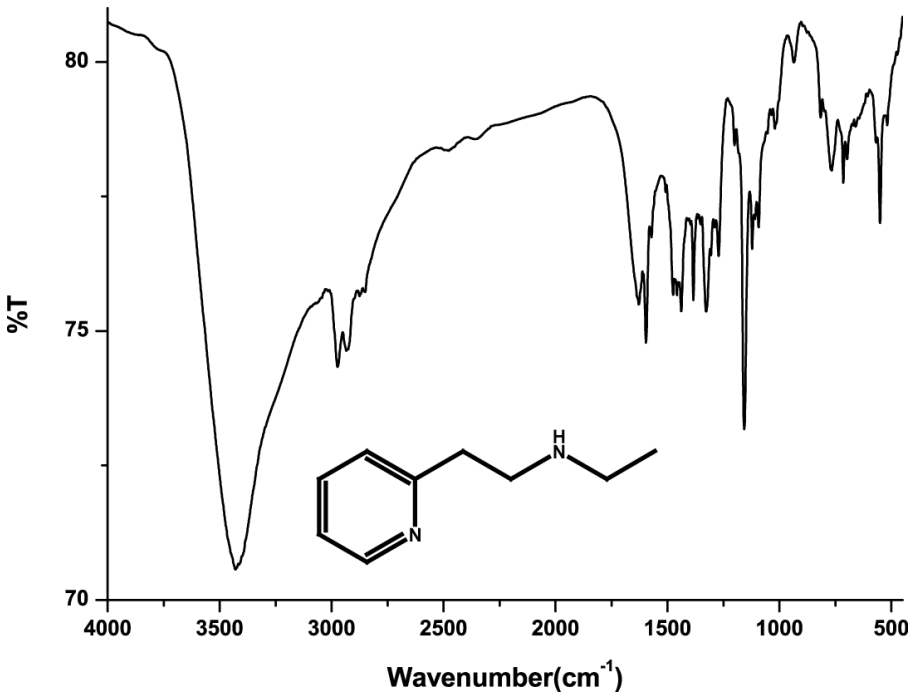

Figure S9: FT-IR spectrum of $\mathbf{L_2}$ in KBr pellet.

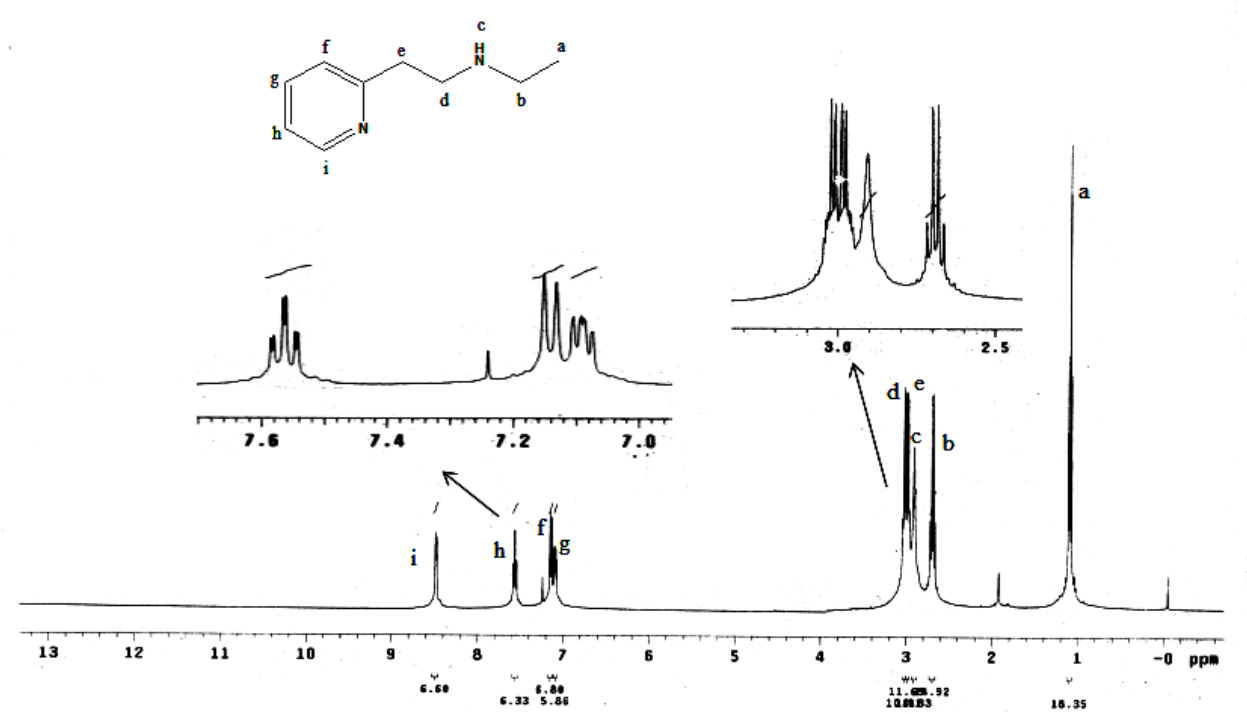

Figure S10: ^{1}H-NMR spectrum of $\mathbf{L_2}$ in $CDCl_3$.

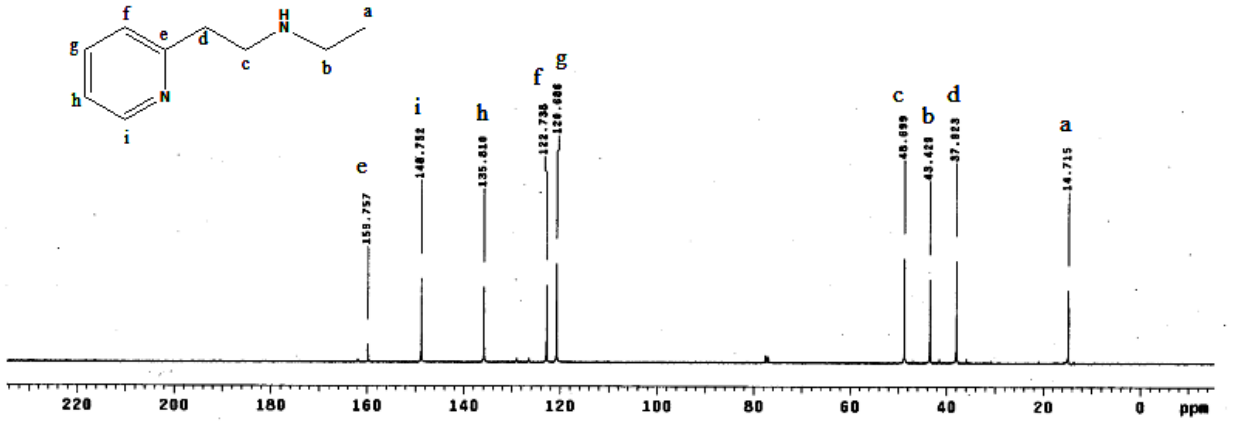

Figure S11: ^{13}C-NMR spectrum of $\mathbf{L_2}$ in $CDCl_3$.

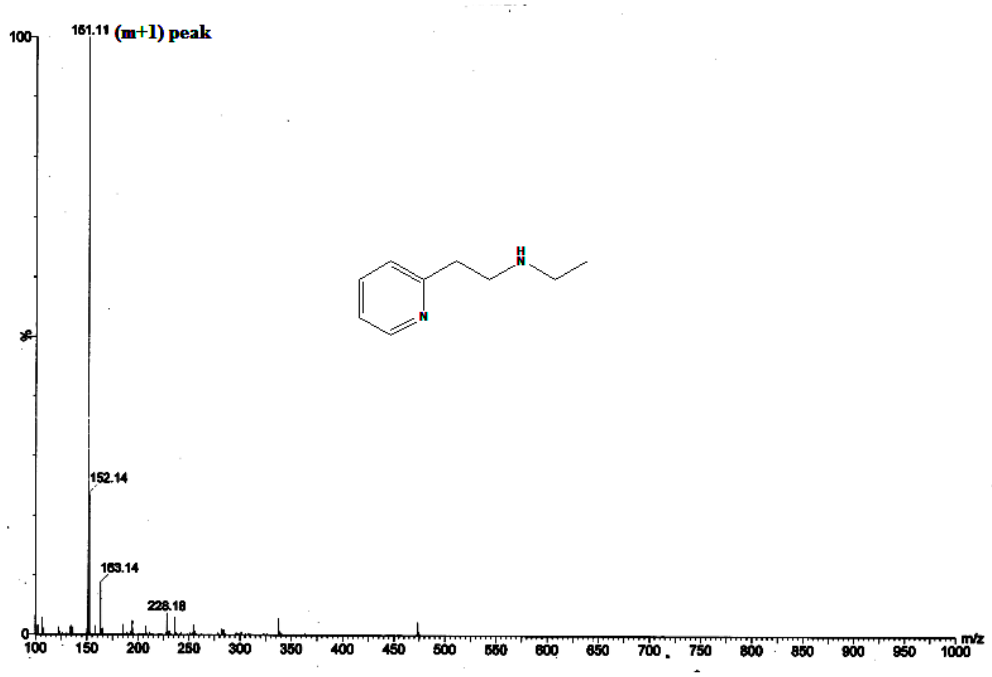

Figure S12: ESI-Mass spectrum of $\mathbf{L_2}$ in methanol.

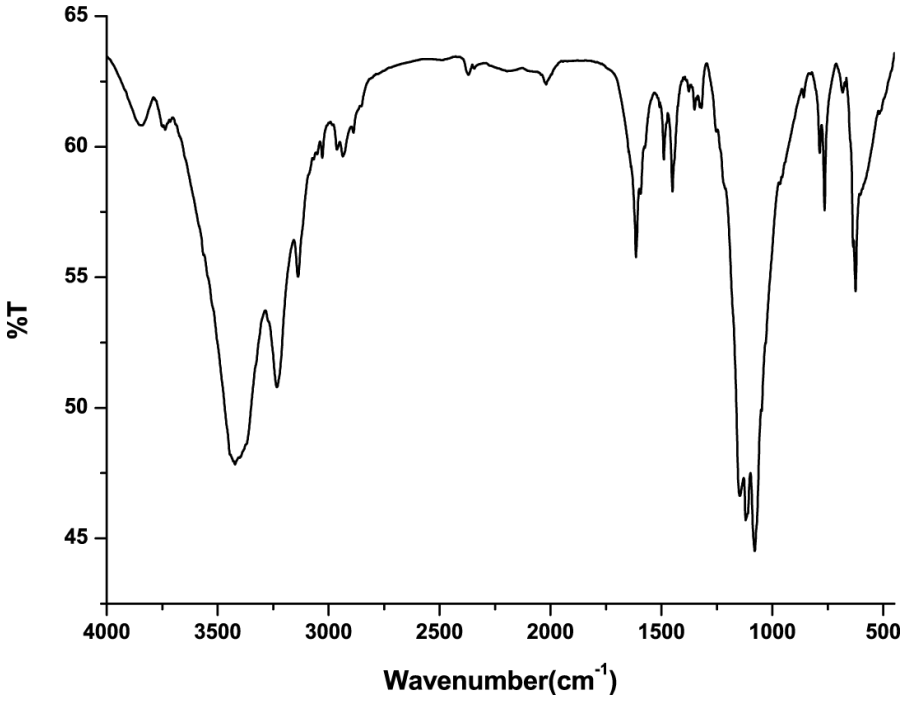

Figure S13: FT-IR spectrum of complex **1** in KBr pellet.

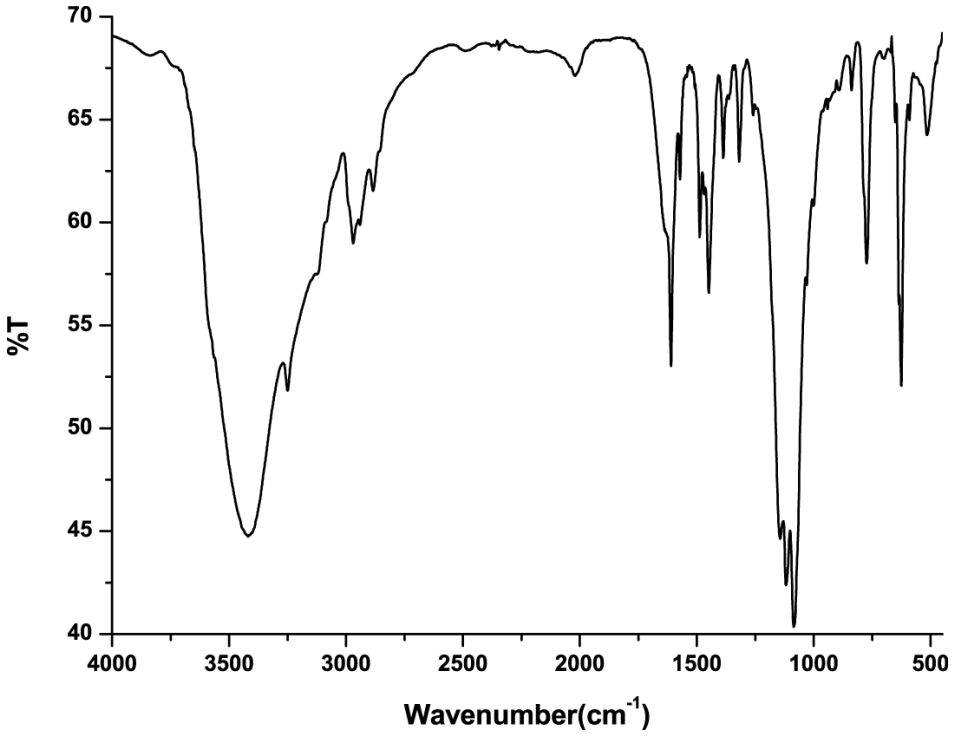

Figure S14: FT-IR spectrum of complex **2** in KBr pellet.

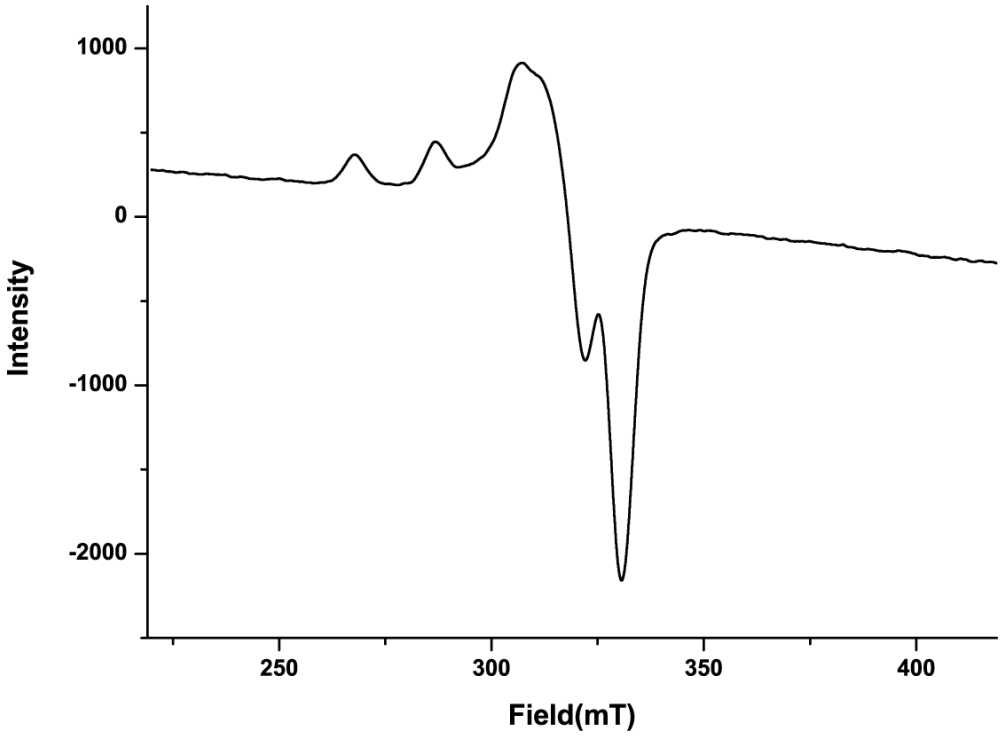

Figure S15: X-Band EPR spectrum of complex **1** in CH_3CN/CH_3OH(50% v/v) at 77K.

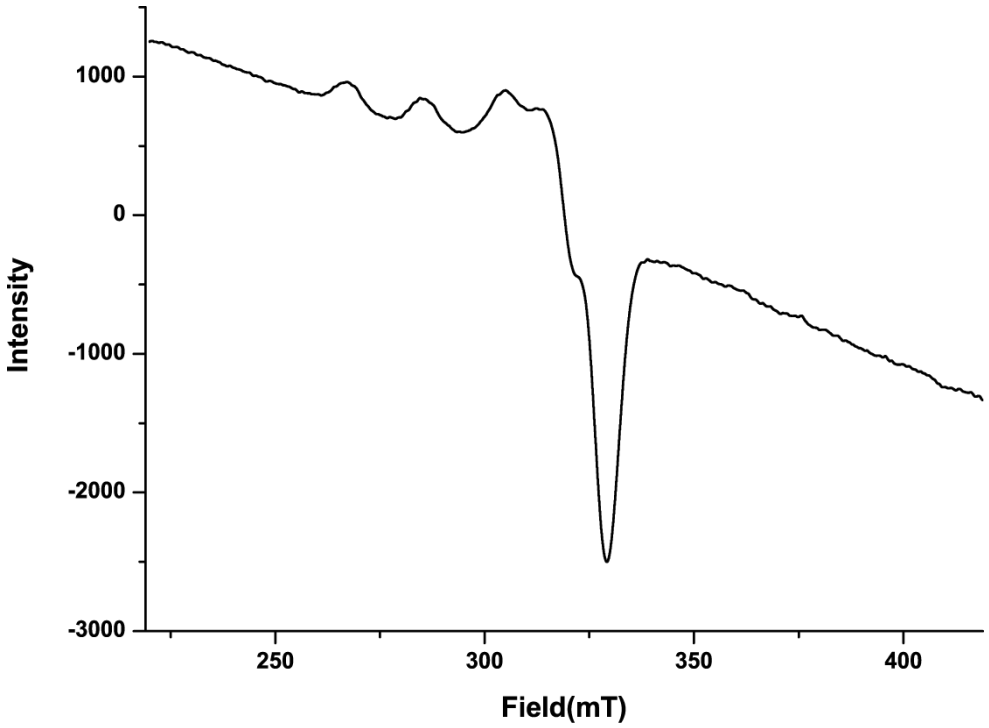

Figure S16: X-Band EPR spectrum of complex **2** in CH_3CN/CH_3OH(50% v/v) at 77K.

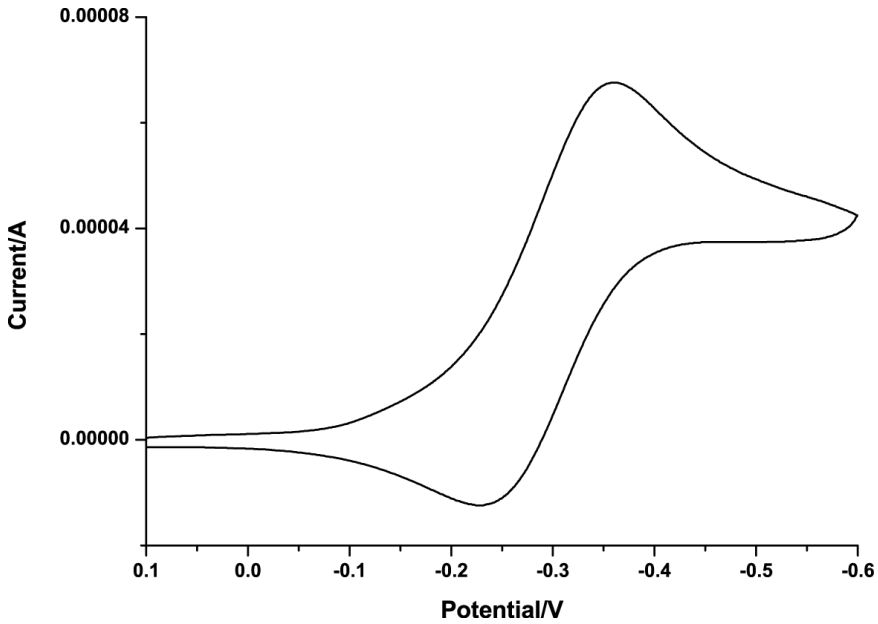

Figure S17: Cyclic voltammogram of complex **1** in acetonitrile. (Tetrabutylammonium perchlorate supporting electrolyte; Pt working and SCE reference electrode and 50 mv/s scan rate).

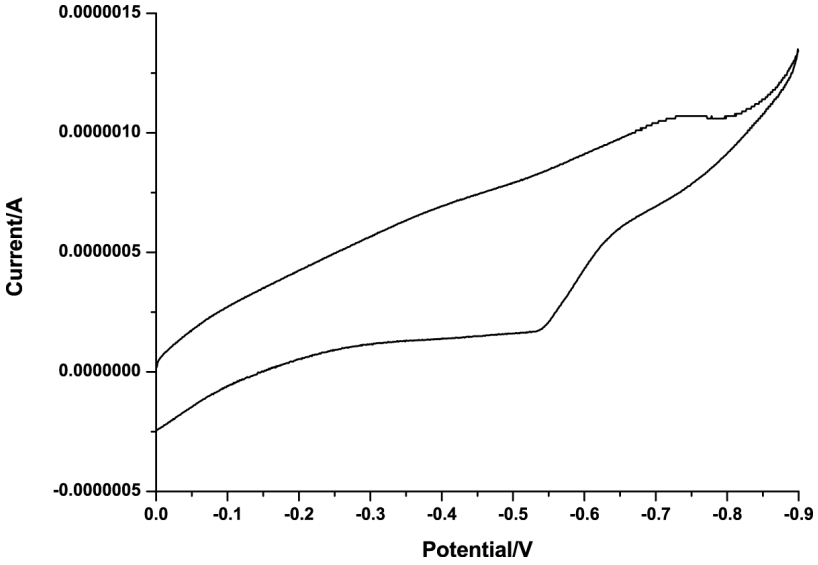

Figure S18: Cyclic voltammogram of complex **2** in acetonitrile. (Tetrabutylammonium perchlorate supporting electrolyte; Pt working and SCE reference electrode and 50 mv/s scan rate).

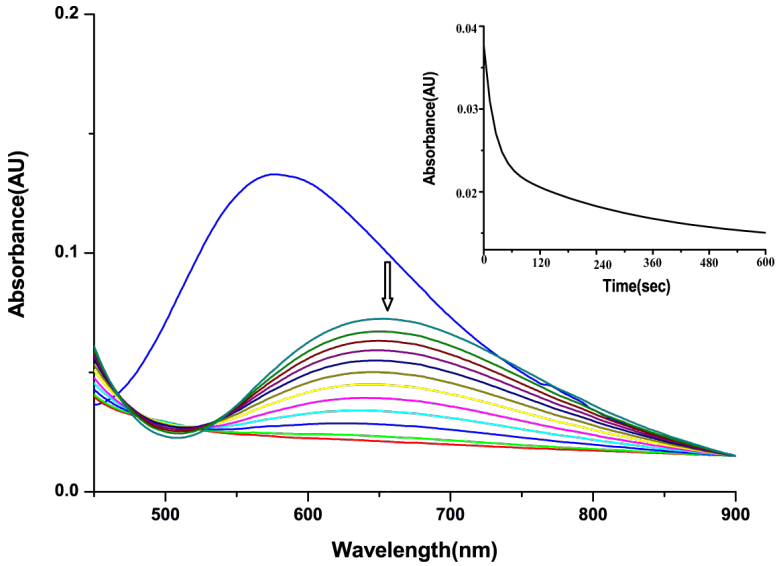

Figure S19: UV-visible spectra of the reaction of complex **1** with nitric oxide in acetonitrile solvent at room temperature. (Blue trace represents the Cu^{II}-species, green represents that of the [Cu^{II}-NO] intermediate which gradually reduced to Cu^{I}-species).{Inset: time scan plots at 650 nm}.

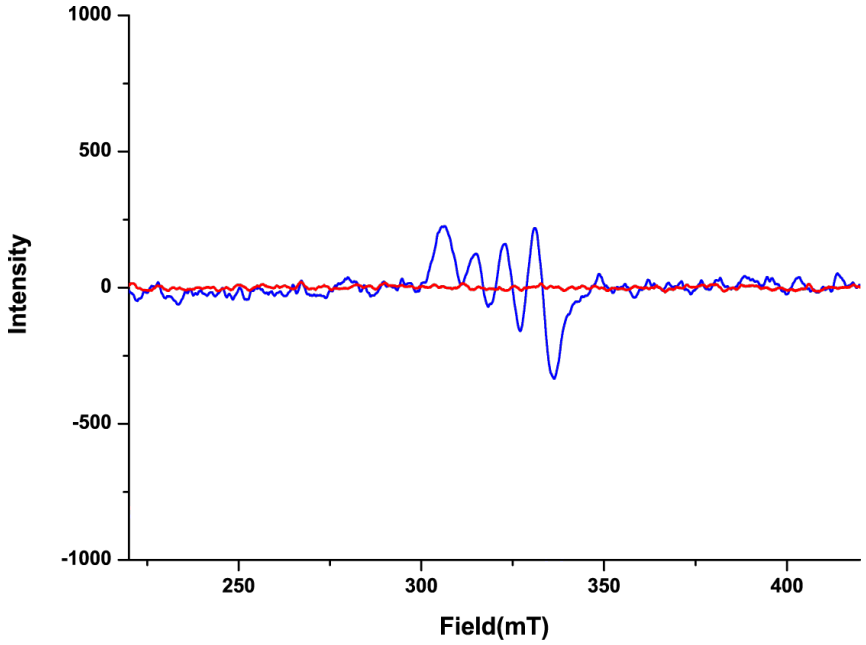

Figure S20: X-Band EPR spectra of complex **1** before (blue trace) and after (red trace) purging NO.

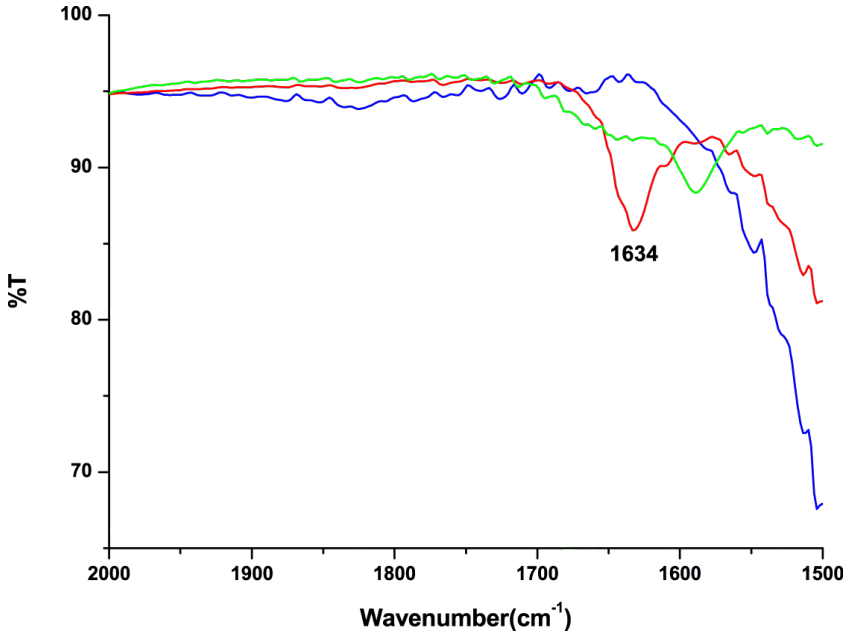

Figure S21: Solution FT-IR spectra complex **1** in acetonitrile. (Blue trace represents solution FT-IR spectrum of complex **1**, red represents that immediately after purging nitric oxide which shows sharp peak at1634 cm^{-1} and green represents that after 10 minutes).

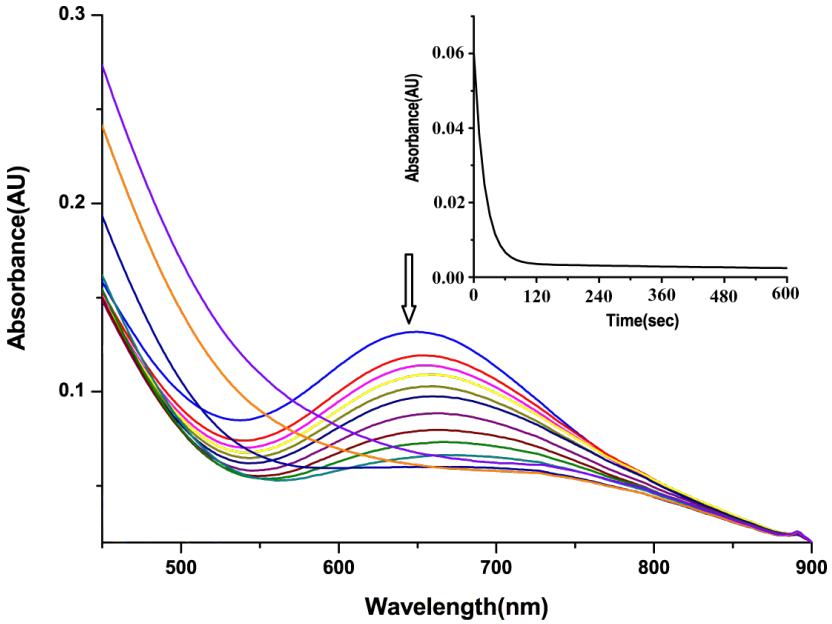

Figure S22: UV-visible spectra of the reaction of complex **2** with nitric oxide in a water solvent at room temperature. (Blue trace represents the Cu^{II}-species, red represents that of the [Cu^{II}-NO] intermediate which gradually reduced to Cu^{I}-species represented by down headed arrow). Inset: Time-scan plot for the decomposition of [Cu^{II}-NO] in water at room temperature.

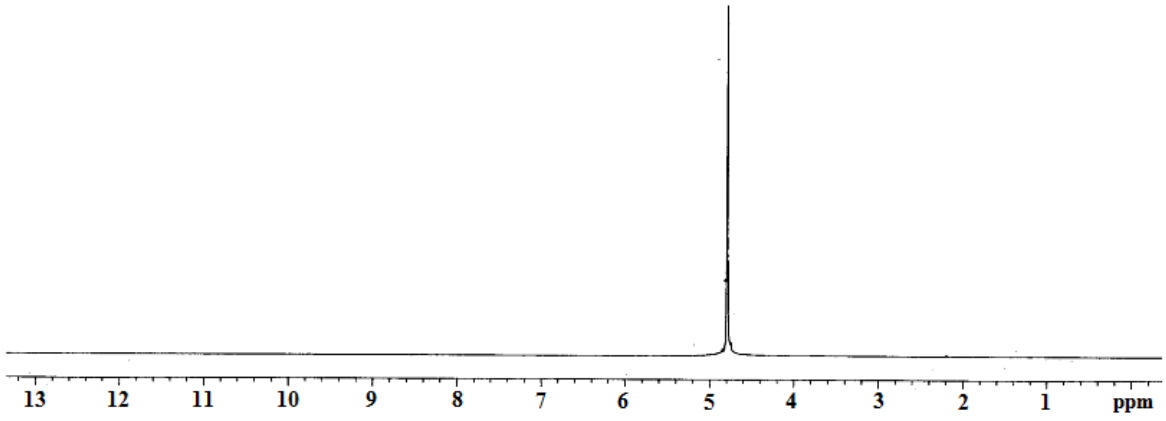

Figure S23: ^{1}H-NMR spectrum of complex **1** in D_2O.

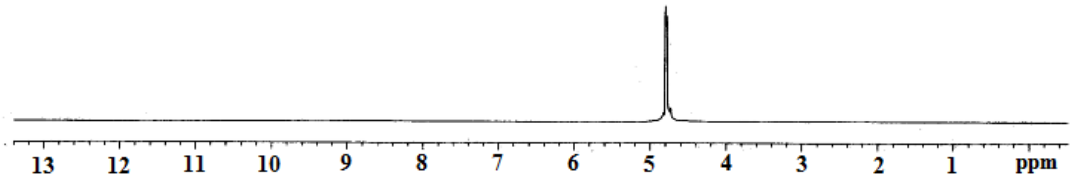

Figure S24: ^{1}H-NMR spectrum of complex **2** in D_2O.

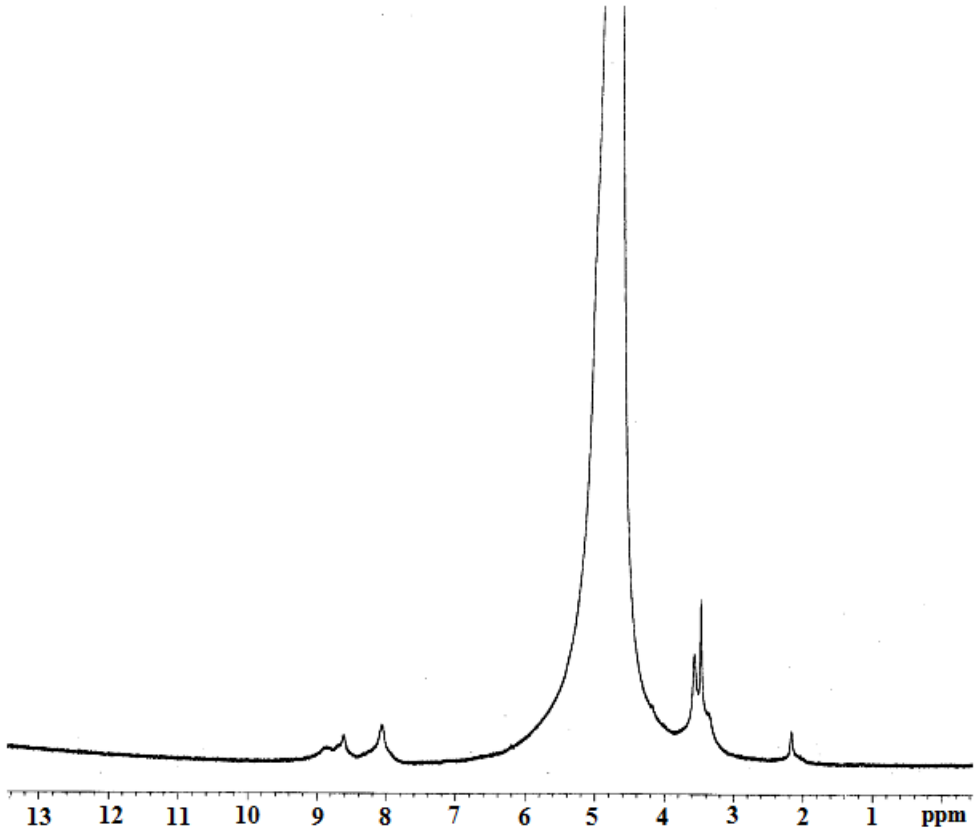

Figure S25: ^{1}H-NMR spectrum of complex **1** in D_2O after the reaction with nitric oxide.

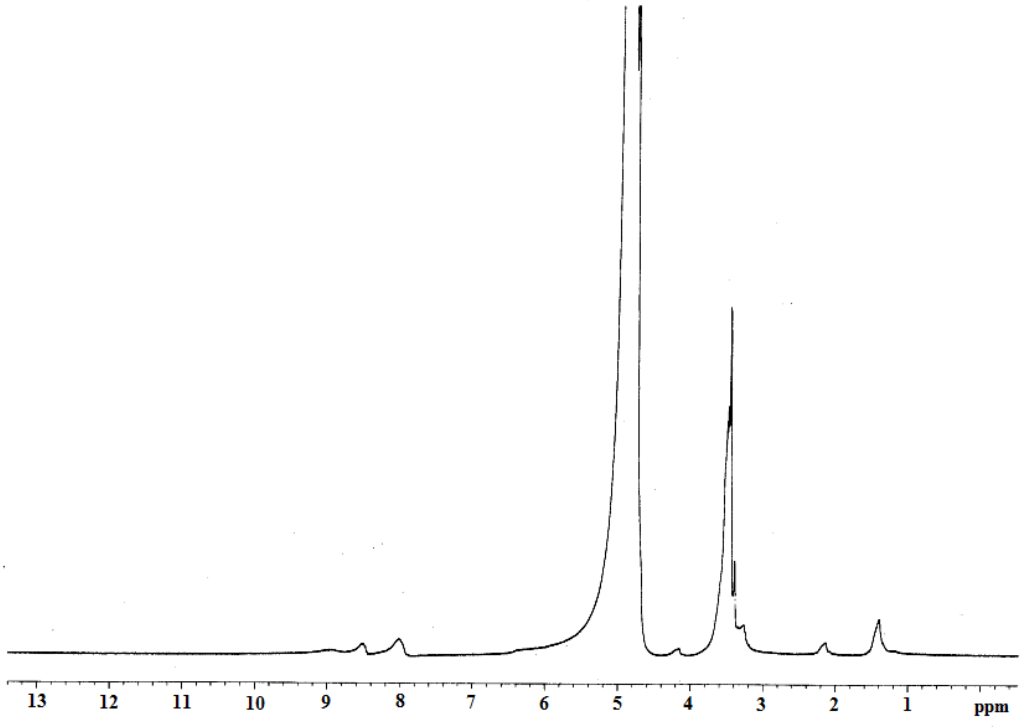

Figure S26: 1H-NMR spectrum of complex **2** in D_2O after the reaction with nitric oxide.

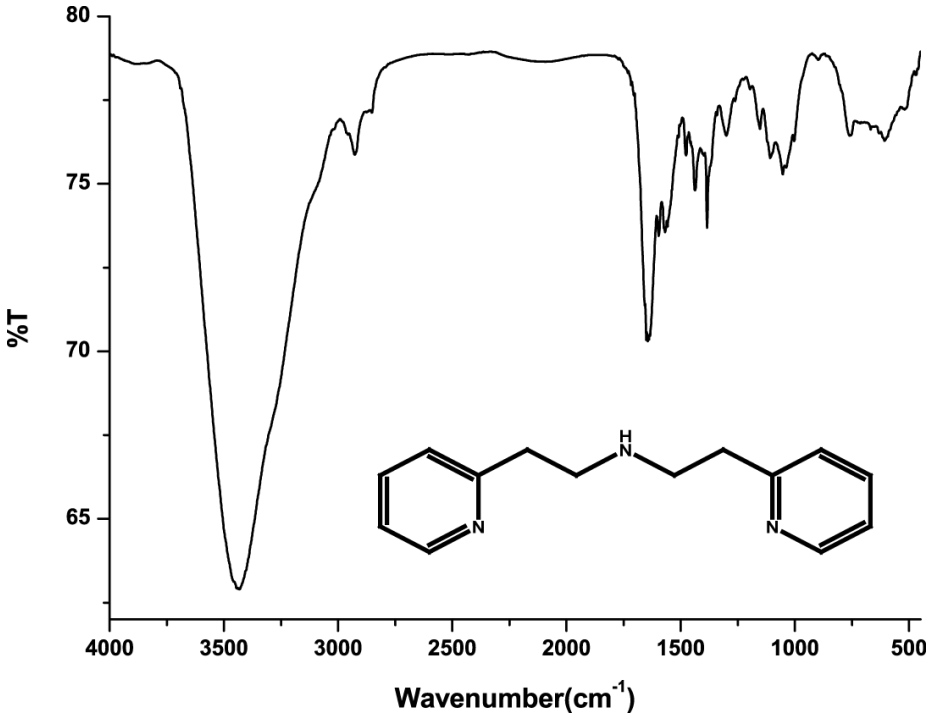

Figure S27: FT-IR spectrum of $\mathbf{L_1}'$ in KBr pellet.

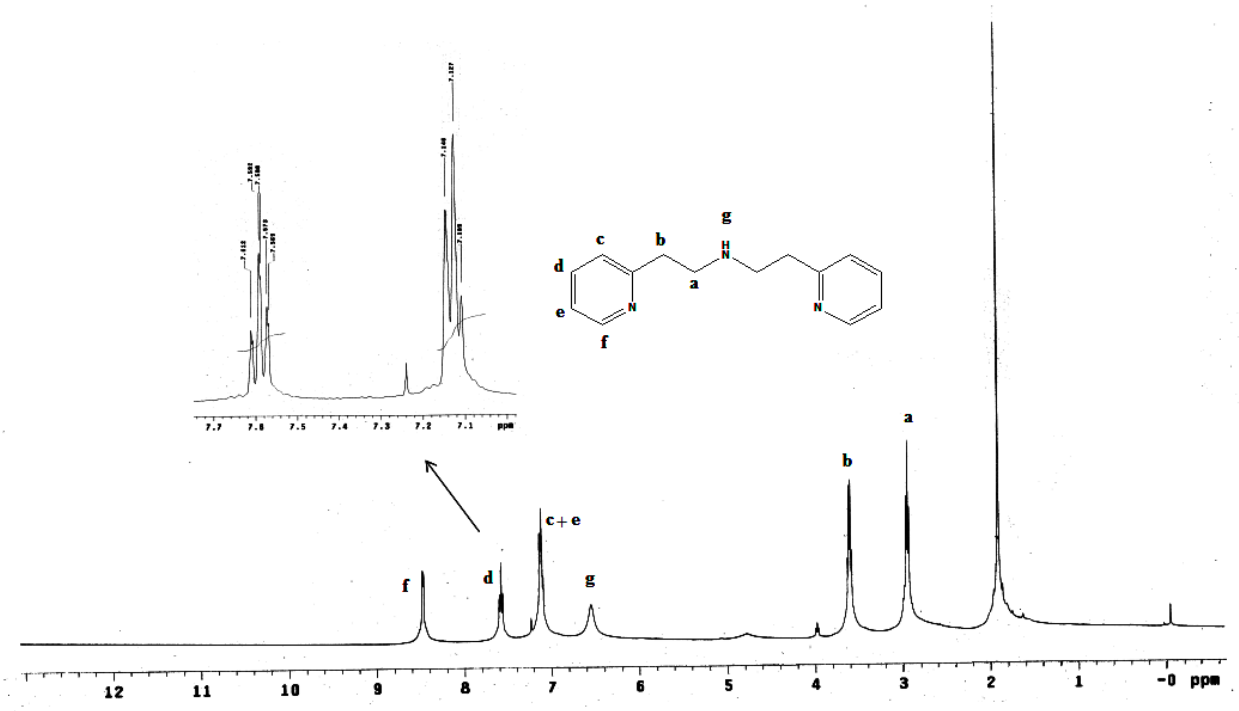

Figure S28: ^{1}H-NMR spectrum of $\mathbf{L_1}'$ of in $CDCl_3$.

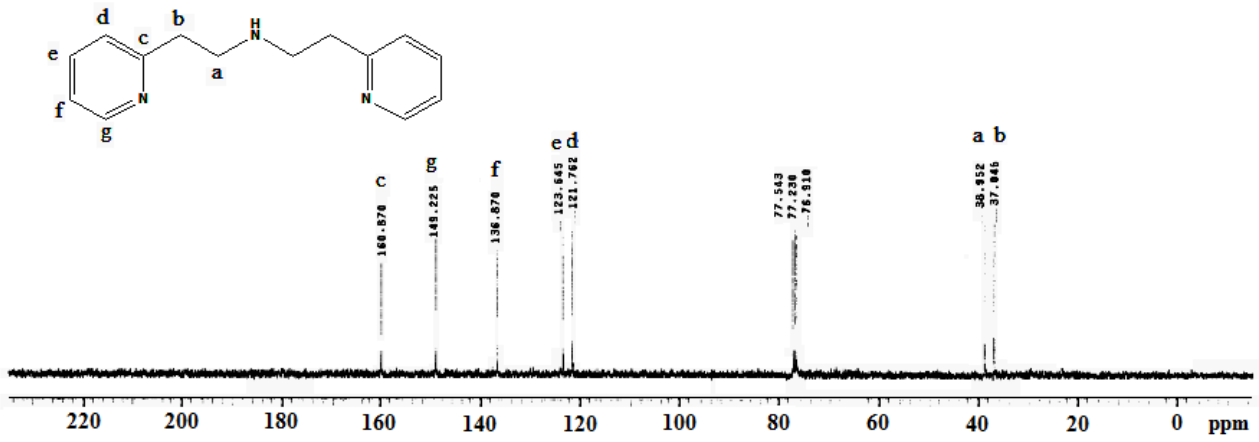

Figure S29: ^{13}C-NMR spectrum of $\mathbf{L_1}'$ of in $CDCl_3$.

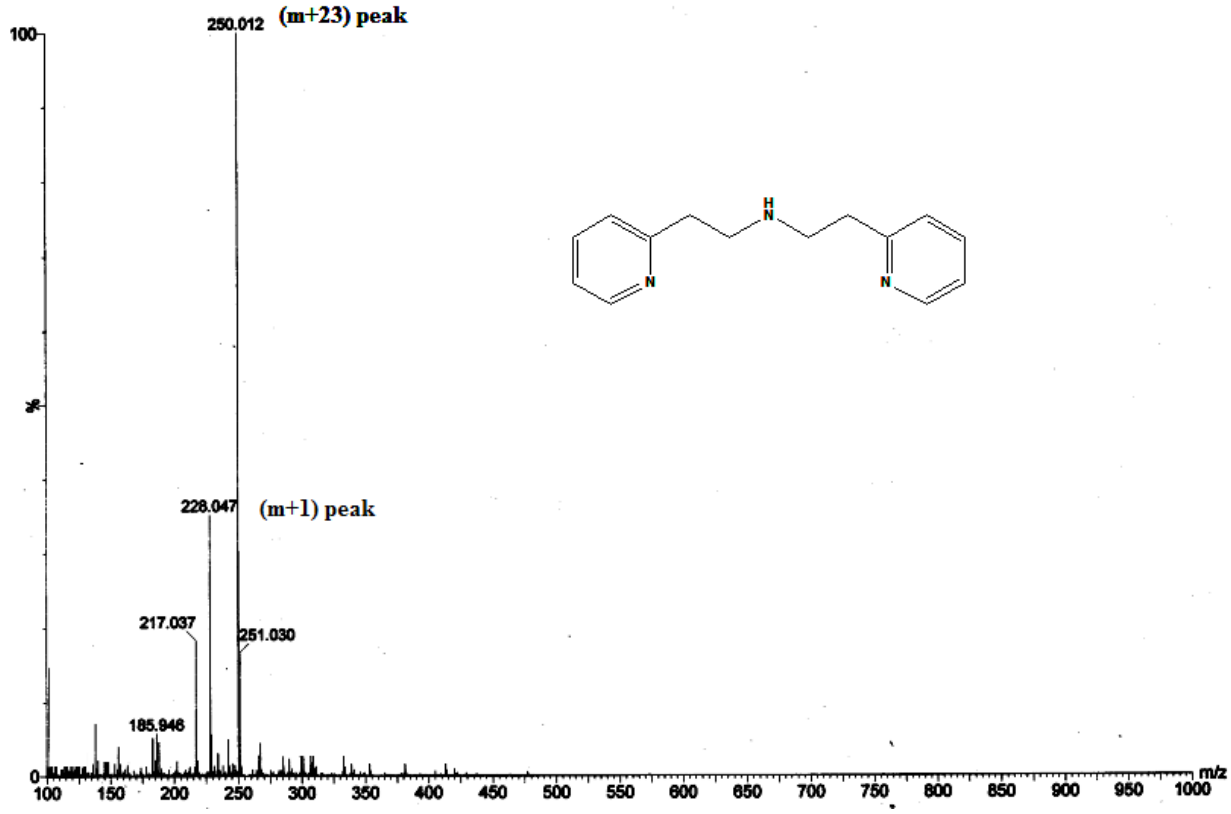

Figure S30: ESI-mass spectrum of $\mathbf{L_1}'$ in methanol.

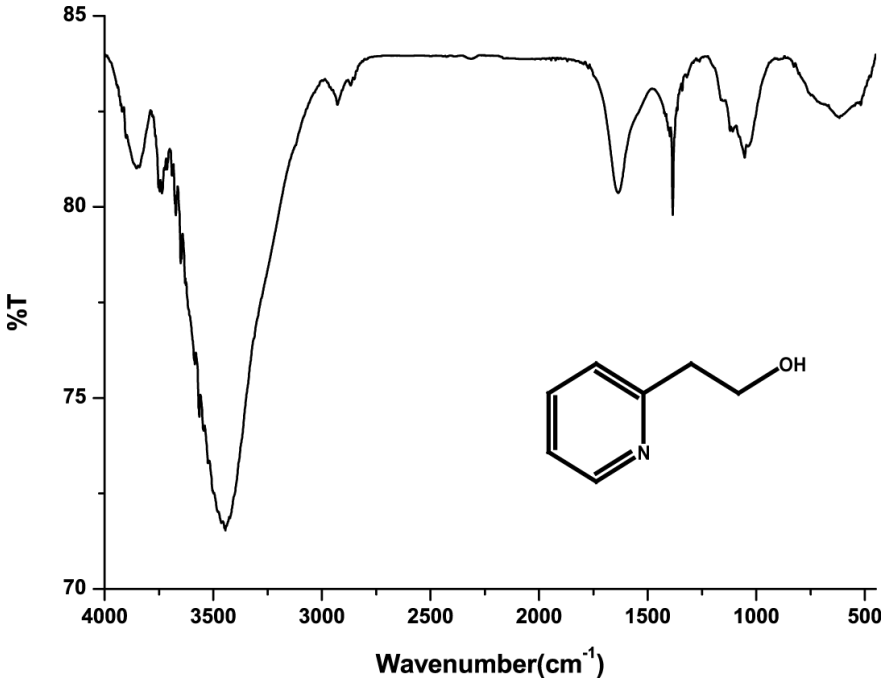

Figure S31: FT-IR spectrum of $\mathbf{L_1}''$ in KBr pellet.

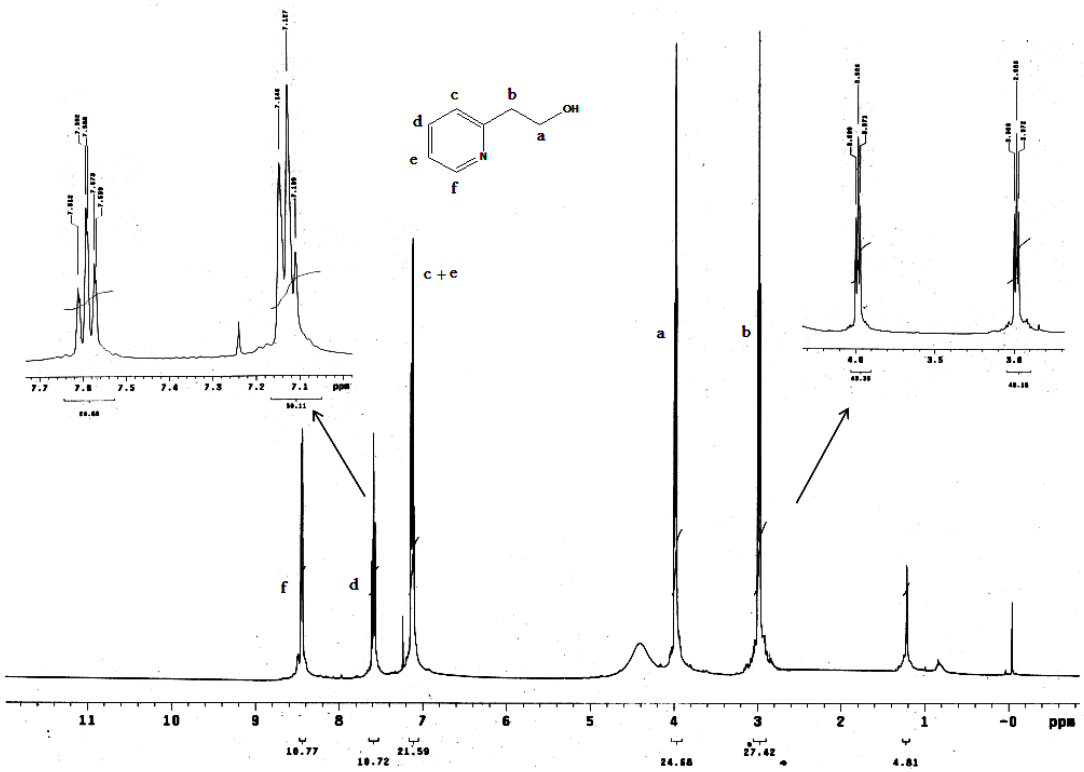

Figure S32: ^{1}H-NMR spectrum of $\mathbf{L_1}^{//}$ of in $CDCl_3$.

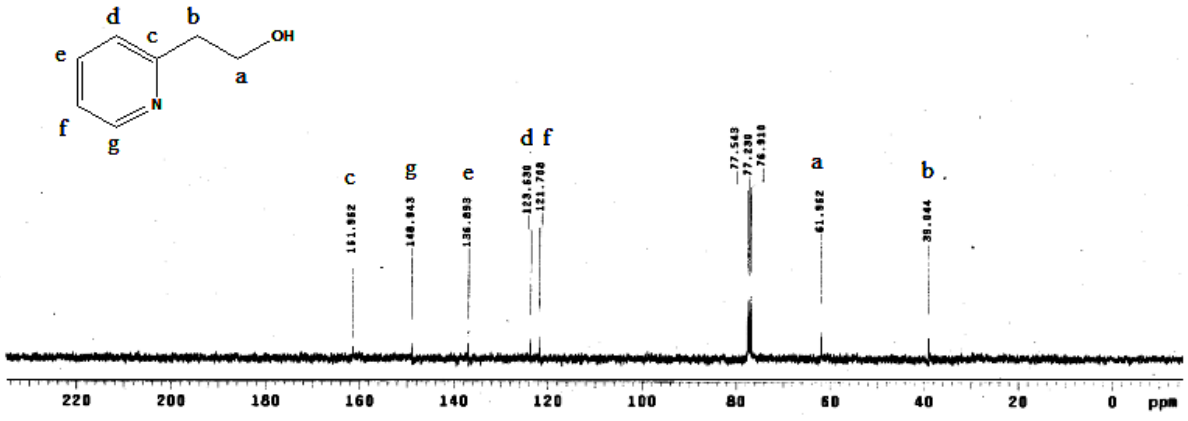

Figure S33: ^{13}C-NMR spectrum of $\mathbf{L_1}^{//}$ of in $CDCl_3$.

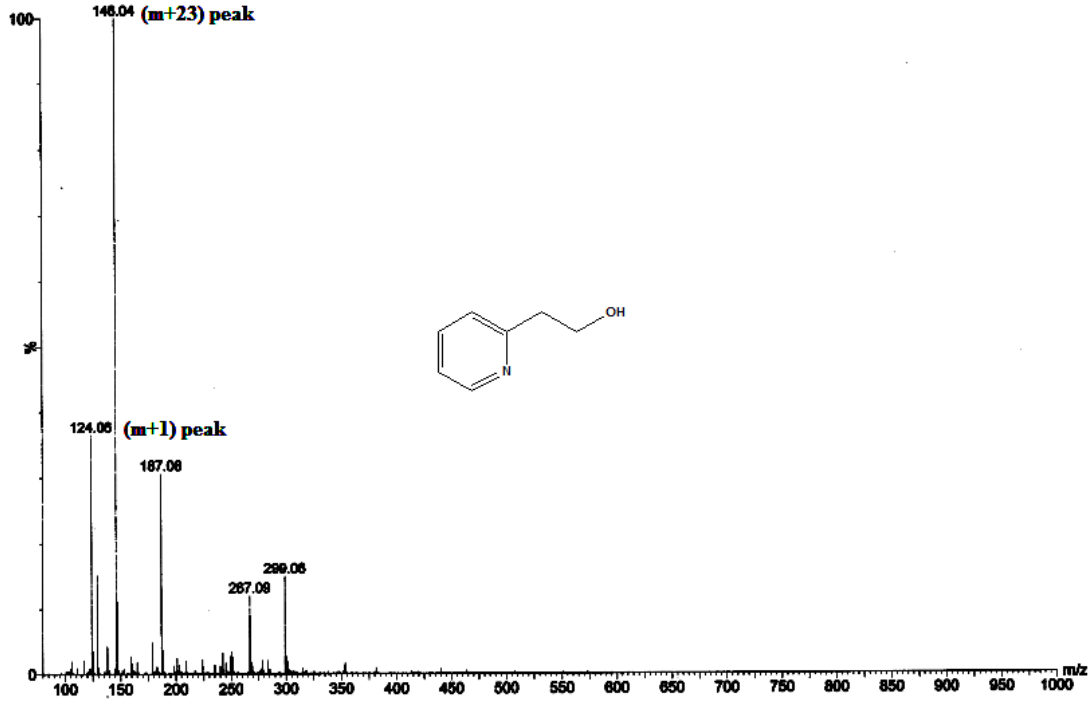

Figure S34: ESI-mass spectrum of $\mathbf{L_1}^{//}$ in methanol.

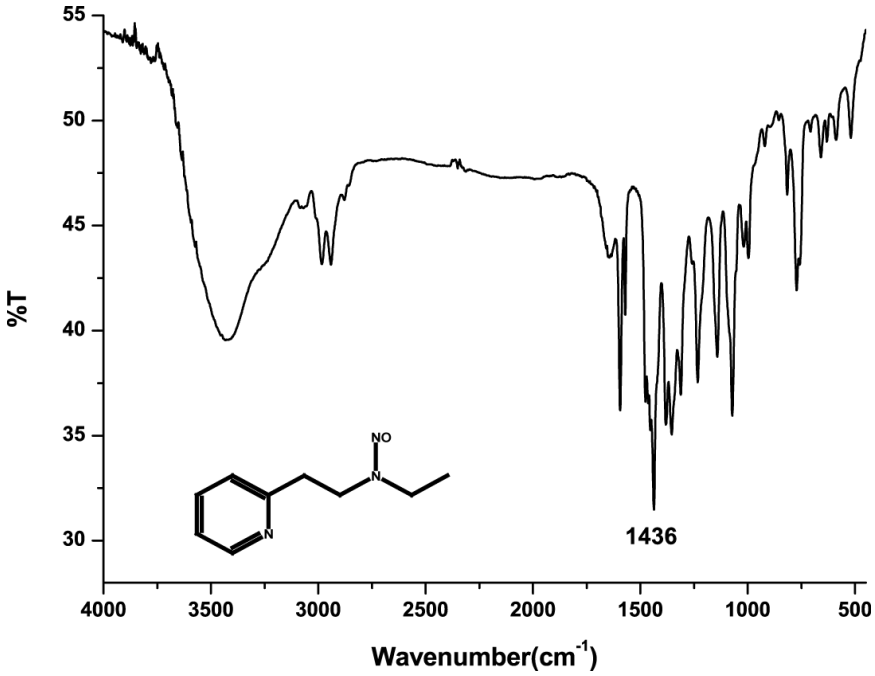

Figure S35: FT-IR spectrum of $\mathbf{L_2}^{/}$ in KBr pellet.

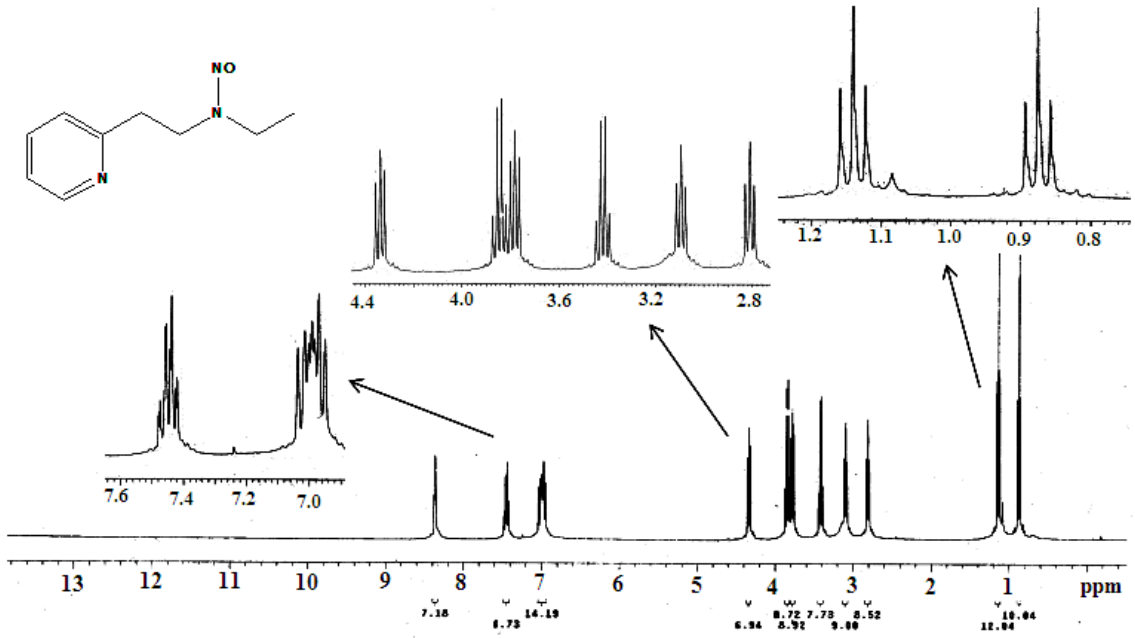

Figure S36: ^{1}H-NMR spectrum of $\mathbf{L_2}'$ of in $CDCl_3$. The presence of extra signals in ^{1}H- and ^{13}C-NMR spectra are due to isomeric impurities.[s1]

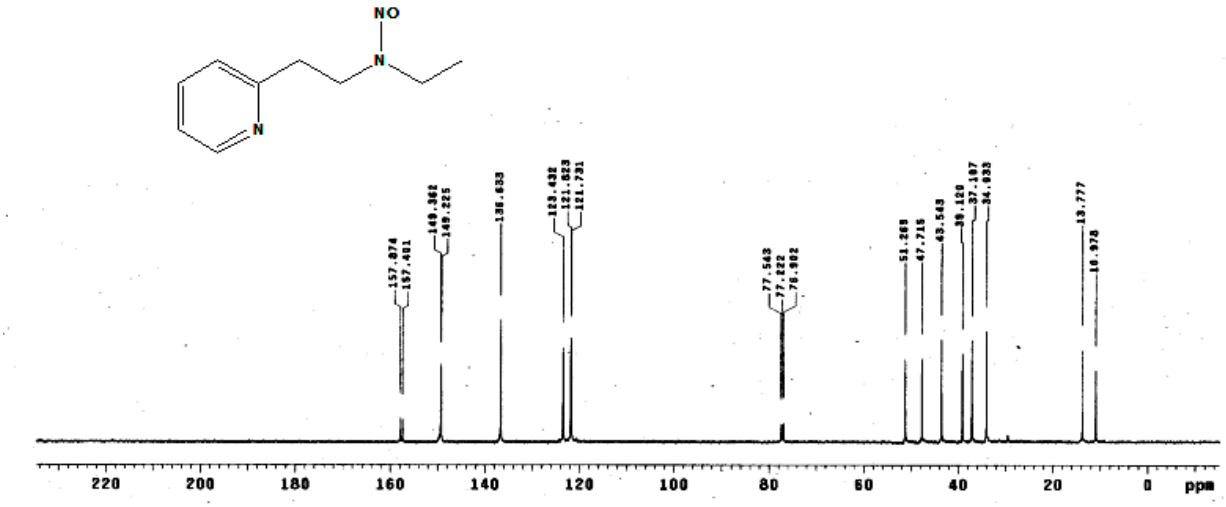

Figure S37: ^{13}C-NMR spectrum of $\mathbf{L_2}'$ of in $CDCl_3$. The presence of extra signals in ^{1}H- and ^{13}C- NMR spectra are due to isomeric impurities.[s1]

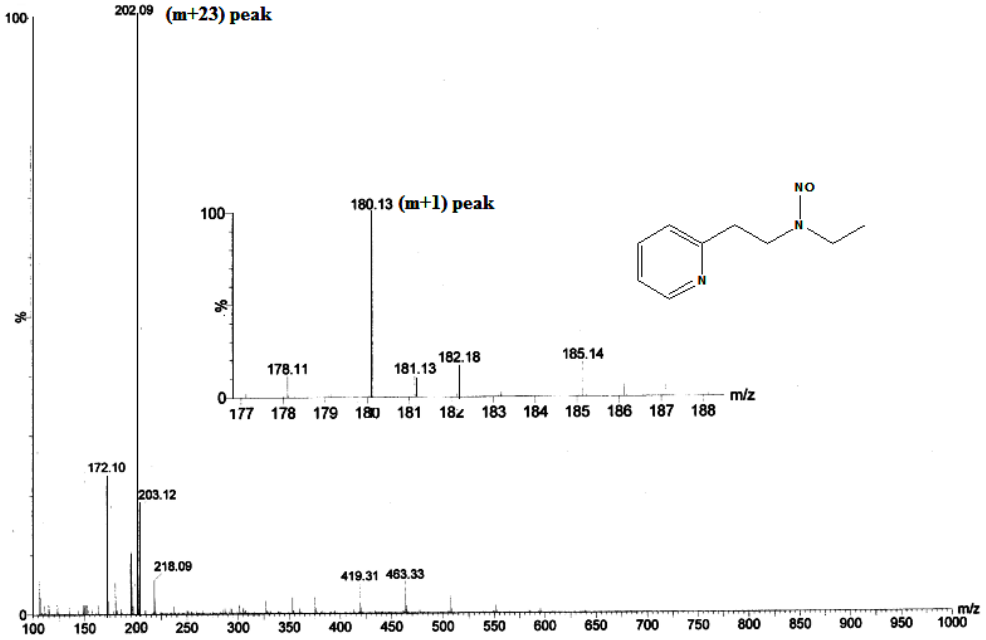

Figure S38: ESI-mass spectrum of $\mathbf{L_2}'$ in methanol.

Table S1: Cartesian coordinates of the calculated geometry of [Cu-NO] intermediate generated from complex **1** and NO

Cu1	1.104093242	-1.333910668	5.786748561
N1	0.936528663	-3.384085015	5.461604025
N2	-0.778673464	-0.784634907	5.065299687
N3	2.906071714	-1.403953012	6.841673630
N4	0.499203755	-0.546915145	7.628808214
C1	-1.683984718	-1.798069668	4.389703687
C2	5.107797347	-2.628722118	7.625020674
H1	5.777048974	-3.551641257	7.623191786
C3	-1.182313986	0.671226584	5.142086794

H2	-0.489148470	1.423462417	5.645281937
C4	3.312804863	-0.161419970	7.583820304
C5	-2.518562571	1.145420357	4.545095363
H3	-2.821115235	2.242317606	4.616611693
C6	2.437963712	1.092504149	7.404174530
H4	2.392887073	1.252619749	6.276267657
H5	2.889742672	2.023389359	7.882810941
C7	5.503612156	-1.387494957	8.448852667
H6	6.462021988	-1.390378093	9.066249539
C8	0.194921659	-3.660052545	4.177572478
H7	0.248803348	-4.783740024	3.993014154
H8	0.688172490	-3.115123346	3.306135395
C9	3.801422573	-2.619368061	6.807078465
H9	3.501827037	-3.533134859	6.194474808
C10	-1.297475480	-3.288714053	4.276840585
H10	-1.798297961	-3.675843529	3.328721153
H11	-1.743148162	-3.845572658	5.166080468
C11	0.982454328	0.869002230	7.876893052
H12	0.903511332	1.044415246	9.000467333
H13	0.327012003	1.627626131	7.333561689
C12	-3.438964102	0.134539681	3.846250994
H14	-4.428332893	0.474733122	3.393637712
C13	4.605016963	-0.137164390	8.417980888
H15	4.900834674	0.800148510	8.995367154

C14	-3.013662554	-1.339665135	3.760547932
H16	-3.686214356	-2.096724489	3.237067771
H17	1.963177946	-3.798558177	5.380004297
H18	0.411859556	-3.871093582	6.309838320
H19	-0.598127505	-0.625852884	7.777129847
H20	1.004532497	-1.180886076	8.386923177
N5	2.010139189	-0.430779506	4.135446868
O1	1.380866006	-0.535226901	2.799873187

Scheme S1: Proposed mechanism of the formation of $\mathbf{L_1}'$

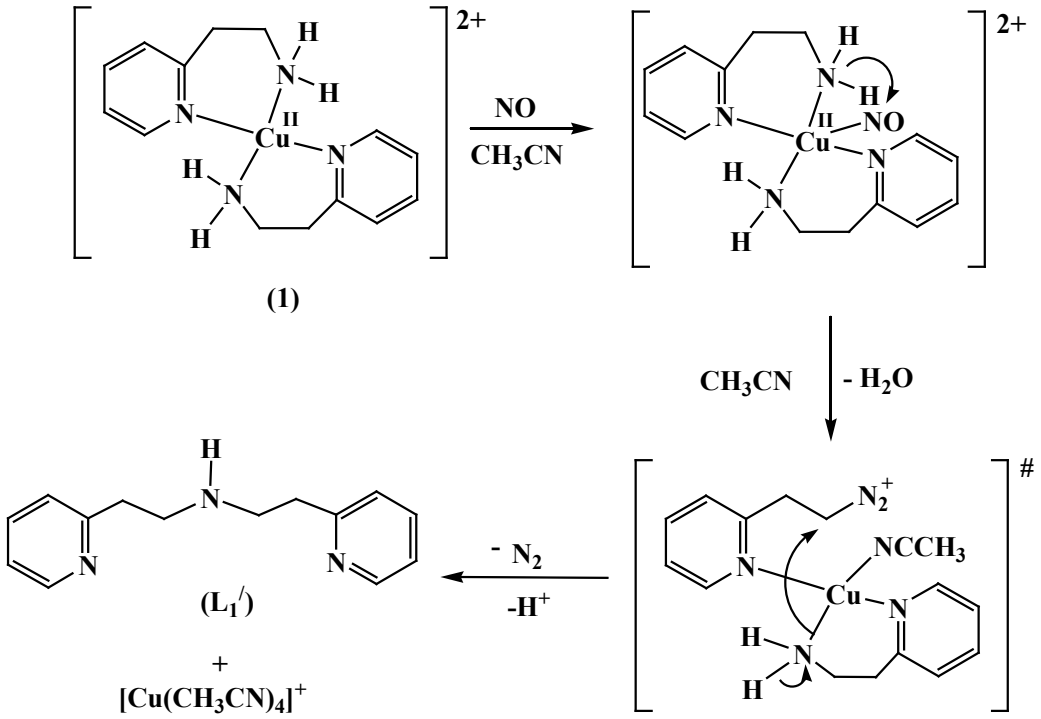

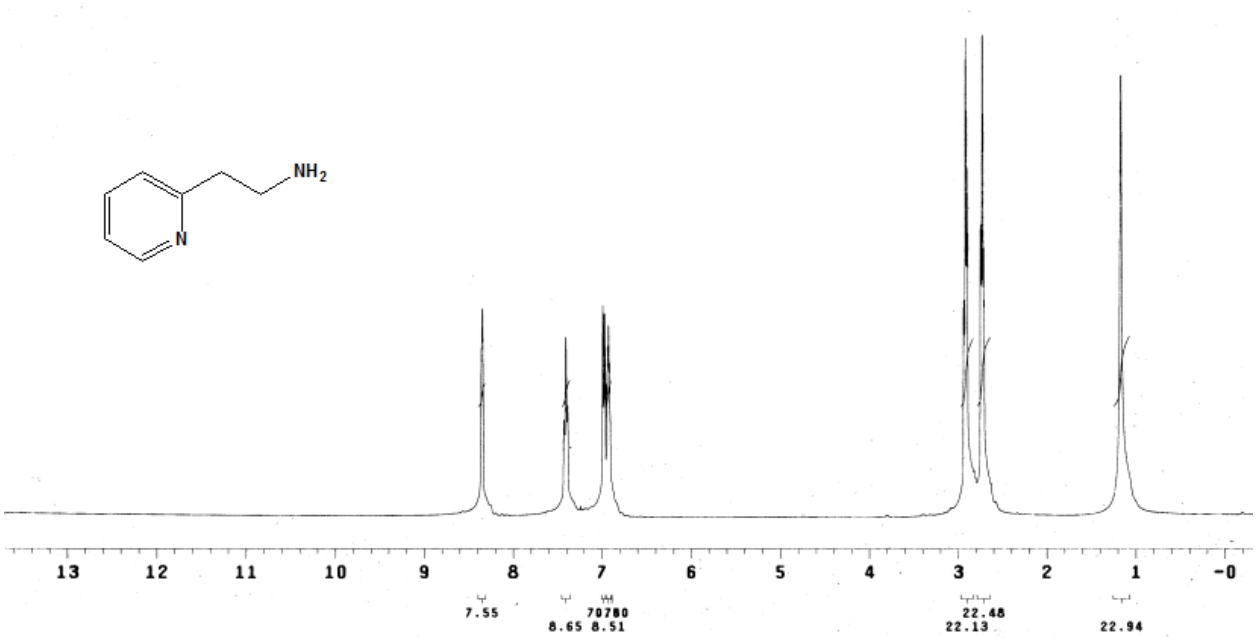

Figure S39: ^{1}H-NMR spectrum of $\mathbf{L_1}$ in $CDCl_3$.

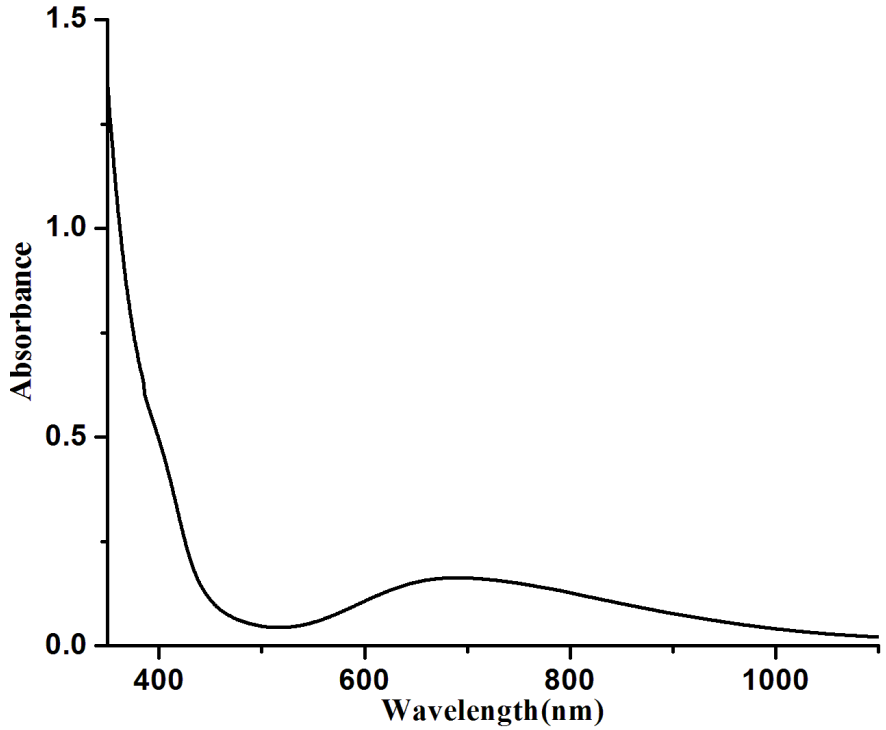

Figure S40: UV-visible spectrum of complex **3** in acetonitrile.

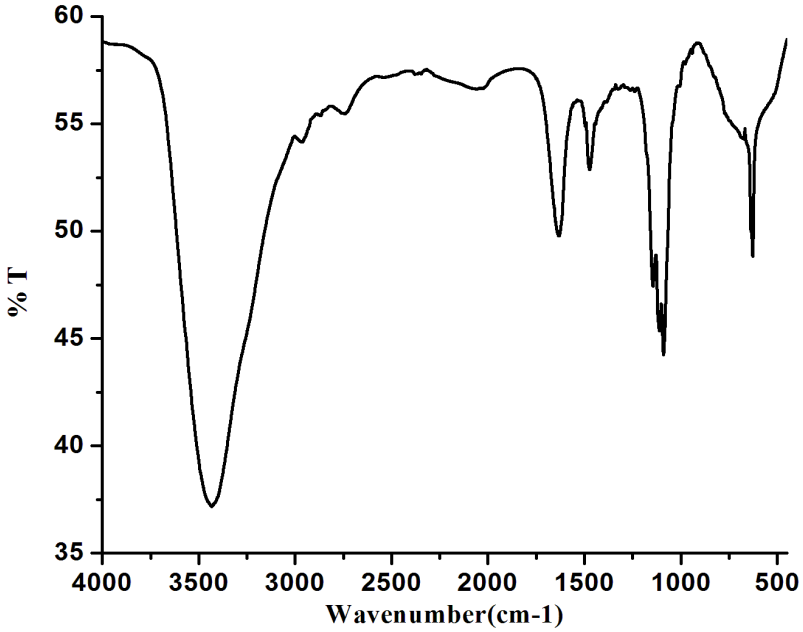

Figure S41: FT-IR spectrum of complex **3** in KBr pellet.

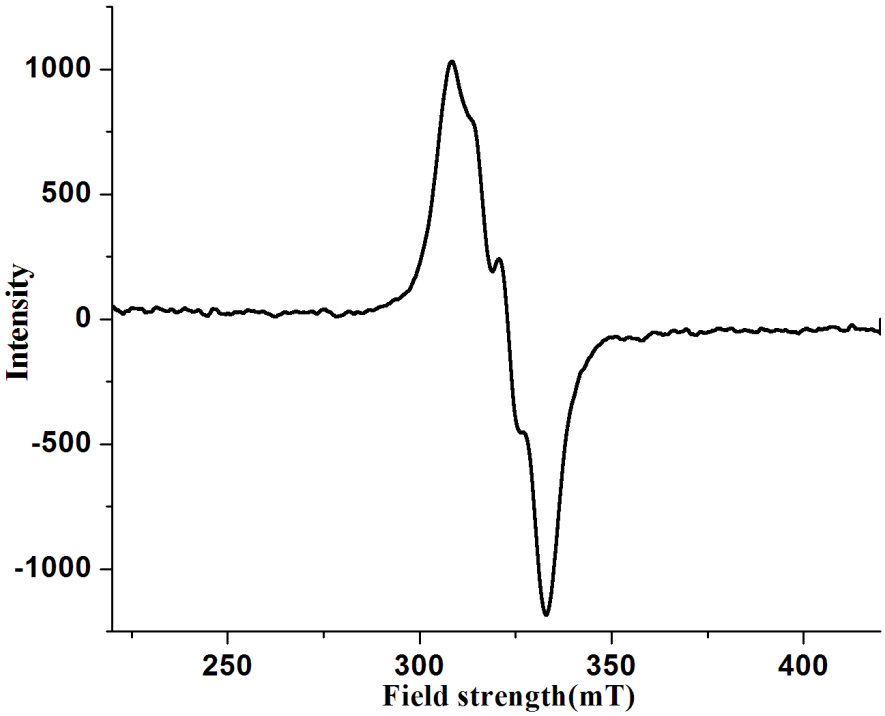

Figure S42: X-band EPR spectrum of complex **3** in acetonitrile at room temperature.

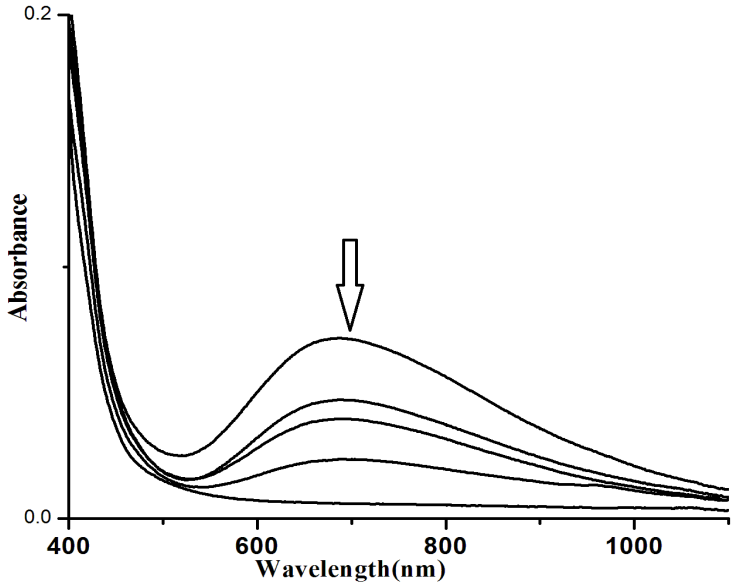

Figure S43: UV-visible study of the reaction of complex **3** with nitric oxide in acetonitrile.

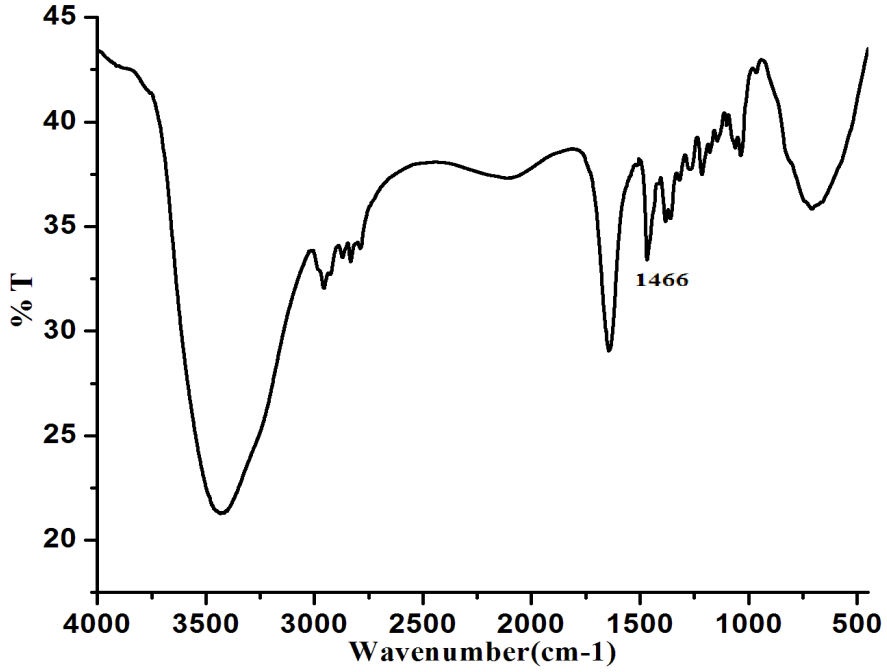

Figure S44: FT-IR spectrum of $\mathbf{L_3}'$ in KBr pellet.

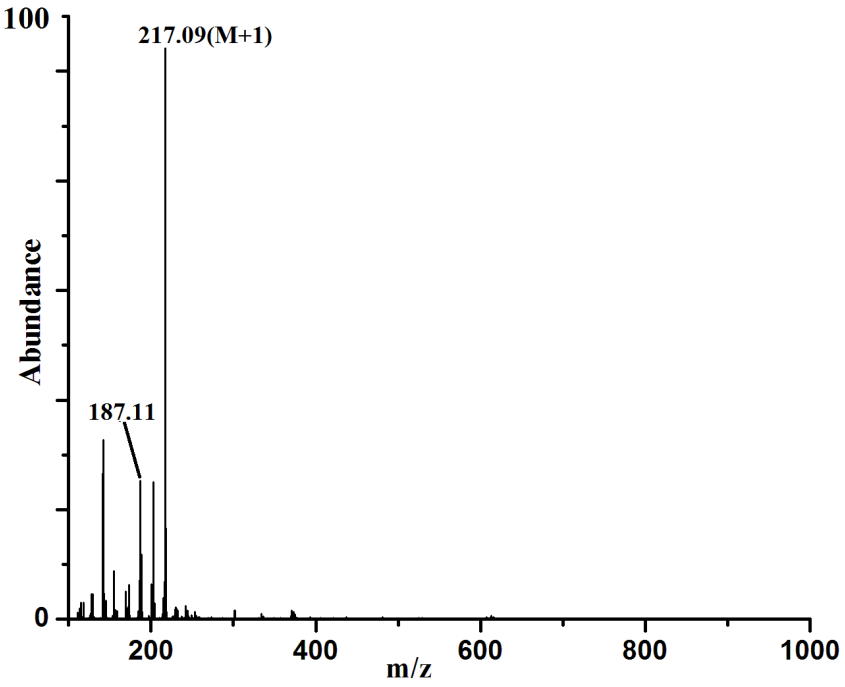

Figure S45: ESI-mass spectrum of $\mathbf{L_3}'$ in methanol.

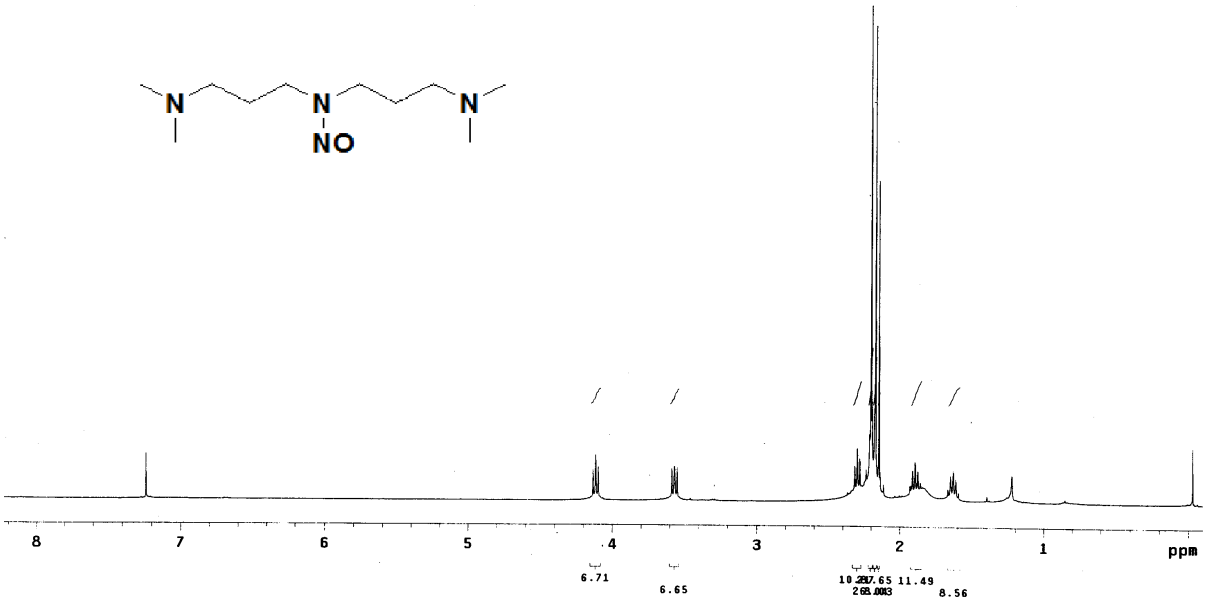

Figure S46: ^{1}H-NMR spectrum of $\mathbf{L_3}'$ in $CDCl_3$.

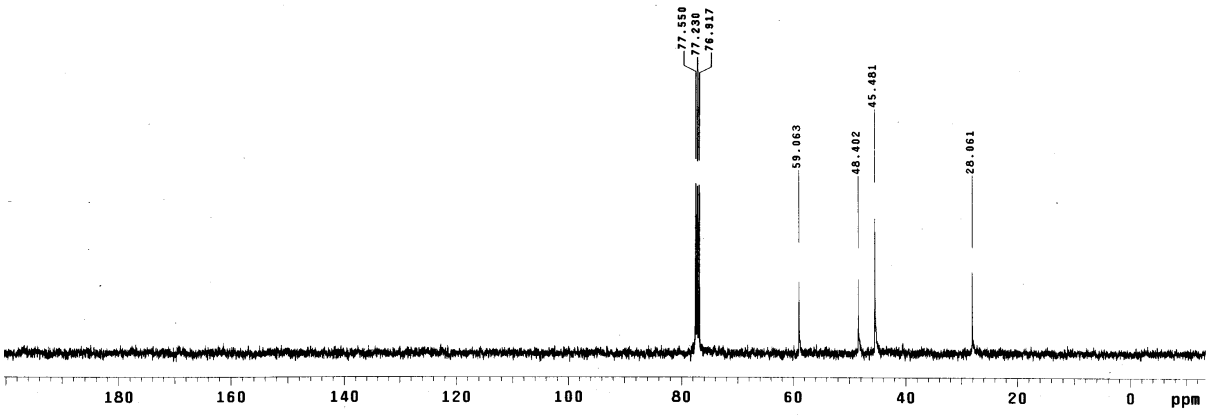

Figure S47: ^{13}C-NMR spectrum of $\mathbf{L_3}'$ in $CDCl_3$.

Reference:

S1. R. K. Harris; R. A. Spragg, *J. Mol. Spect.* 1969, **30**, 77.